A novel RyR1 inhibitor prevents and rescues sudden death in a mouse model of malignant hyperthermia and heat stroke

Toshiko Yamazawa[1†*], Takuya Kobayashi[2†], Nagomi Kurebayashi[2†], Masato Konishi[2], Satoru Noguchi[3], Takayoshi Inoue[4], Yukiko U. Inoue[4], Ichizo Nishino[3], Shuichi Mori[5], Hiroto Iinuma[5], Noriaki Manaka[5], Hiroyuki Kagechika[5], Arkady Uryas[6], Jose Adams[6], Jose R. Lopez[7], Xiaochen Liu[8], Christine Diggle[8], Paul D. Allen[8], Sho Kakizawa[9], Keigo Ikeda[10], Bangzhong Lin[10], Yui Ikemi[10], Kazuto Nunomura[10], Shinsaku Nakagawa[10], Takashi Sakurai[2], Takashi Murayama[2*]

[1]Department of Molecular Physiology, Jikei University School of Medicine, Tokyo, Japan.

[2]Department of Pharmacology, Juntendo University School of Medicine, Tokyo, Japan.

[3]Department of Neuromuscular Research, National Institute of Neuroscience, National Center of Neurology and Psychiatry, Tokyo, Japan.

[4]Department of Biochemistry and Cellular Biology, National Institute of Neuroscience, National Center of Neurology and Psychiatry, Tokyo, Japan.

[5]Institute of Biomaterials and Bioengineering, Tokyo Medical and Dental University, Tokyo, Japan.

[6]Department of Neonatology, Mount Sinai Medical Center, Miami, FL, USA.

[7]Department of Research, Mount Sinai Medical Center, Miami, FL, USA.

[8]Leeds Institute of Biomedical & Clinical Sciences, School of Medicine, University of Leeds, St James's University Hospital, Leeds, UK.

[9]Department of Biological Chemistry, Graduate School of Pharmaceutical Sciences, Kyoto University, Kyoto, Japan

[10]Center for Supporting Drug Discovery and Life Science Research, Graduate School of

Pharmaceutical Science, Osaka University, Suita, Japan.

[†]These authors contributed equally to this work.

Corresponding author: Takashi Murayama (takashim@juntendo.ac.jp), Toshiko Yamazawa (toshiko1998@jikei.ac.jp)

Abstract

Mutations in the type 1 ryanodine receptor (RyR1), a Ca^{2+} release channel in skeletal muscle, hyperactivate the channel to cause malignant hyperthermia (MH) and are implicated in severe heat stroke. Dantrolene, the only approved drug for MH, has the disadvantages of having very poor water solubility and long plasma half-life. We show here that a novel RyR1-selective inhibitor, 6,7-(methylenedioxy)-1-octyl-4-quinolone-3-carboxylic acid (Compound 1, Cpd1), effectively prevents and treats MH and heat stroke in several mouse models relevant to MH. Cpd1 reduced resting intracellular Ca^{2+}, inhibited halothane- and isoflurane-induced Ca^{2+} release, suppressed caffeine-induced contracture in skeletal muscle, reduced sarcolemmal cation influx, and prevented or reversed the fulminant MH crisis induced by isoflurane anesthesia and rescued animals from heat stroke caused by environmental heat stress. Notably, Cpd1 has great advantages of better water solubility and rapid clearance *in vivo* over dantrolene. Cpd1 has the potential to be a promising new candidate for effective treatment of patients carrying RyR1 mutations.

Introduction

The type 1 ryanodine receptor (*RYR1*; MIM# 180901) is a Ca^{2+}-release channel in the sarcoplasmic reticulum (SR) of skeletal muscle that plays a central role in muscle contraction[1,2].

51 During excitation-contraction (E-C) coupling, RyR1 releases Ca^{2+} through physical association
52 with the sarcolemmal slow voltage gated Ca^{2+} channel (dihydropyridine receptor, DHPR)
53 during depolarization of T-tubule membrane. This mechanism is referred to as depolarization-
54 induced Ca^{2+} release (DICR) [3, 4]. The RyR1 channel can also be directly activated by Ca^{2+},
55 which is referred to as Ca^{2+}-induced Ca^{2+} release (CICR) [5, 6], although its importance in the
56 function is much lower than RyR2 and RyR3 [7].

57 Genetic mutations in the *RYR1* gene are associated with malignant hyperthermia
58 (MH; MIM# 145600) [8]. MH is a life-threatening disorder characterized by skeletal muscle
59 rigidity and elevated body temperature in response to all volatile anesthetics such as halothane
60 or isoflurane [9]. MH mutations are thought to hyperactivate CICR, which causes massive Ca^{2+}
61 release by halogenated anesthetics under resting conditions [6, 10, 11]. Heat stroke is a medical
62 emergency with a high body temperature and altered mental status, which is triggered by
63 exercise or environmental heat stress [12, 13]. It has been reported that MH mutations in the *RYR1*
64 gene are also implicated in some heat stroke [14, 15, 16].

65 The only drug approved for ameliorating the symptoms of MH is dantrolene [17, 18].
66 Dantrolene was first developed in 1960s as a muscle relaxant [19] and was later shown to prevent
67 Ca^{2+} release by direct interaction with RyR1 [20, 21]. However, dantrolene has several
68 disadvantages for clinical use: the main disadvantage is its poor water solubility which makes
69 rapid preparation difficult in emergency situations [22]. In addition, dantrolene has long plasma
70 half-life ($t_{1/2}$ ~12 h), which causes long-lasting side effects such as muscle weakness [23]. To date,
71 no alternative drugs improving these disadvantages have been developed over 40 years since
72 the first discovery.

73 We have recently identified oxolinic acid as a novel RyR1-selective inhibitor with
74 better water solubility using efficient high-throughput screening platform for RyR1 inhibitors
75 [24, 25]. We synthesized a series of oxolinic acid derivatives by structural development, and

successfully identified 6,7-(methylenedioxy)-1-octyl-4-quinolone-3-carboxylic acid (Compound 1, Cpd1) with extremely high potency which is comparable to dantrolene in *in vitro* study [26]. In this study, we tested whether Cpd1 has therapeutic effects in treating the MH crisis in a novel MH mouse model carrying *RYR1*-p.R2509C, a corresponding mutation (p.R2508C) in humans [27, 28] and two other MH mouse models, *RYR1*-p.R163C [29] and *RYR1*-p.G2435R [30]. We found that Cpd1 effectively prevents and reverses a fulminant MH crisis triggered by isoflurane anesthesia. The drug also treats mice with heat stroke caused by environmental heat stress. A notable finding is that Cpd1 is rapidly metabolized in mice. Our results provide crucial evidence for Cpd1 as a RyR1 inhibitor that may prove to be clinically-useful.

Results

Generation of novel MH model mice carrying *RYR1*-p.R2509C mutation

A MH mouse model carrying p.R2509C mutation in the *RYR1* gene (*RYR1*-p.R2509C) was created using CRISPR/Cas9 system (see Materials and Methods, **Fig. 1a**). An additional *Xba* I site was introduced to screen the genotype by PCR-RFLP. The homozygous *RYR1*-p.R2509C mice died in late embryonic stage, but heterozygous *RYR1*-p.R2509C mice grew normally and were as fertile as wild type (WT) (**Fig. 1b**).

It has previously been shown when MH susceptible mice, swine or humans with mutations in the *RYR1* gene are exposed to volatile anesthetics, it causes a MH crisis and if untreated can lead to death [29, 30, 31, 32, 33, 34]. When anesthetized by isoflurane, nearly 80% (68 out of 83) heterozygous *RYR1*-p.R2509C (R2509C) mice rapidly increased their rectal temperature to over 40°C (42.3±1.3°C, n=16) (**Fig. 1c, d**), exhibited muscle rigidity (**Fig. 1c, inset**) and died within 90 min (64±30 min, n=16) from start of exposure (**Fig. 1e**). In the remaining R2509C mice, exposure to isoflurane caused an increase in rectal temperature but it did not exceed 39°C. In contrast, WT mice showed no elevation in rectal temperature in

101 response to isoflurane (**Fig. 1c, 1d**). Elevation of rectal temperature looks two-phase reaction;
102 it rose slowly at first and then surged around 39°C (**Fig. 1c**). Interestingly, time from rectal
103 temperature of 39°C to death was quite similar among all individual mice (16±4 min, n=16)
104 (**Fig. 1e**). We further investigated sex difference in response to isoflurane. More male mice
105 (90%) succumbed to isoflurane than females (65%) (**Fig. 1f**). Among the mice that succumbed,
106 there was no significant sex difference in the rectal temperature (**Fig. 1g**) and time to death (**Fig.**
107 **1h, 1i**). These findings suggest that *RYR1*-p.R2509C mice can reproduce human MH symptoms
108 in response to exposure to volatile anesthetics and thus are a useful model for test of Cpd1.
109

110 **Effect of Cpd1 on intracellular Ca^{2+} homeostasis in the isolated single muscle cells**

111 Cpd1 is a derivative of oxolinic acid with an octyl group at nitrogen atom (oxolinic acid has an
112 ethyl group) [26]. This modification increased the potency for inhibiting the RyR1 channel nearly
113 70-fold in a HEK293 cell-based assay (IC_{50} values from 810 nM for oxolinic acid to 12 nM for
114 Cpd1). Since Cpd1 is a free acid, it is virtually water insoluble. We therefore prepared its
115 sodium salt, which neutralizes the carboxyl group and significantly increases water solubility
116 (**Fig. 2a**). The Cpd1 sodium salt exhibited good solubility in normal saline (0.9% NaCl) as well
117 as pure water and glucose solution (**Table 1**). In contrast, dantrolene sodium salt was soluble
118 in pure water and glucose solution but hardly soluble in normal saline, which is in accord with
119 previous studies [35].

120 We initially tested the effect of Cpd1 in *in vitro* experiments using enzymatically-
121 isolated single flexor digitorum brevis (FDB) muscle cells from the R2509C mice. Abnormal
122 resting intracellular Ca^{2+} ($[Ca^{2+}]_i$) homeostasis in skeletal muscle cells is one of the most
123 common features associated with MH in susceptible humans [36], swine [31, 32], and MH model
124 mice [29, 30, 33, 34]. Muscle cells were loaded with a fluorescent Ca^{2+} indicator, Cal520, and $[Ca^{2+}]_i$
125 was fluorometrically monitored during exposure of the cells to halothane, which is used for

126 clinical MH testing [37]. Whereas halothane up to 0.1% (v/v) did not change $[Ca^{2+}]_i$ in WT cells,
127 it caused increase in $[Ca^{2+}]_i$ in R2509C cells in a dose-dependent manner (**Fig. 2b, 2c**).
128 Pretreatment of R2509C cells with Cpd1 (100 nM) reduced resting $[Ca^{2+}]_i$ (**Supplementary**
129 **Fig. 1a, 1b**) and completely abolished halothane induced increases in $[Ca^{2+}]_i$ (**Fig. 2b, 2c**). We
130 then used the ratiometric Ca^{2+} indicator fura-2 to estimate the unstimulated resting $[Ca^{2+}]_i$ and
131 whether or not it could be modified by Cpd1. At rest fura-2 F_{340}/F_{380} ratios were significantly
132 higher in R2509C cells than in WT and Cpd1 reduced $[Ca^{2+}]_i$ in R2509C cells in a dose-
133 dependent manner but had no significant effect on WT (**Fig. 2d**). Similar to the effects of
134 halothane, exposure to isoflurane increased $[Ca^{2+}]_i$ in R2509C but not in WT cells and Cpd1
135 completely prevented this effect. (**Fig. 2e, 2f**).

136 It has been shown that sarcolemmal cation influx is accelerated in skeletal muscle of
137 several MH model mice compared with WT mice [38, 39]. This is due to enhanced sarcolemmal
138 Ca^{2+} entry in response to chronic reduced SR Ca^{2+} load. We therefore measured resting Mn^{2+}
139 quench of fura-2 fluorescence. Unexpectedly, rate of Mn^{2+} quench in R2509C was not different
140 from WT and in this model Cpd1 had no effect (**Supplementary Fig. 2a, 2b**).

141

142 **Effect of Cpd1 on contraction force in isolated muscles**

143 The In Vitro Contracture Test (IVCT) using muscle biopsies is widely used for
144 diagnosis of MH susceptibility in humans [40]. A subject is considered MH positive if the muscle
145 exhibited a greater contracture at a lower dose of caffeine or halothane. We therefore tested the
146 effect of Cpd1 on caffeine-induced contracture in soleus muscles isolated from *RYR1*-p.R2509C
147 mice. WT muscles showed only minimal contracture in responses to caffeine up to 20 mM (**Fig.**
148 **3a**). In contrast, R2509C muscles exhibited dose-dependent contracture during exposure to
149 caffeine and pretreatment with 3 μM Cpd1 decreased caffeine-induced contracture tension of
150 R2509C muscles at 20 mM caffeine (**Fig. 3b**).

151 It has been reported that soleus muscles from MH model mice exhibit heat-induced
152 increase in the basal force at temperatures of 35°C or higher [33]. Basal tension at 42°C was
153 significantly increased in R2509C solei compared to WT muscles (**Fig. 3c, 3d**) and pretreatment
154 with 3 μM Cpd1 significantly reduced the heat-induced contracture in R2509C muscles.
155 Dantrolene is known to suppress twitch and tetanic contractions in both normal and
156 MH muscles [41, 42]. We tested whether Cpd1 affects twitch and tetanic contractions and whether
157 or not there was a difference in the Cpd1 effect between MH and WT. Untreated soleus muscles
158 from both WT and R2509C mice showed similar twitch and tetanic contraction force and
159 treatment with 3 μM Cpd1 significantly reduced both twitch and tetanic contraction force in
160 both groups (**Fig. 3e-3g**). The effect was stronger on twitch (72% inhibition) (**Fig. 3f**) than on
161 tetanic (35% inhibition at 100 Hz) (**Fig. 3g**) contractions, which is similar to dantrolene [41].
162
163 **Effect of Cpd1 on *in vivo* isoflurane challenge**
164 We next tested whether Cpd1 can prevent or treat MH episodes in R2509C mice *in*
165 *vivo*. We first tested the preventive effect of Cpd1 on MH episodes in response to isoflurane
166 exposure. We used male mice for the experiments, since male mice were more sensitive to
167 isoflurane than female mice (see **Fig. 1f**). Doses of either 3 mg/kg or 10 mg/kg of Cpd1
168 solubilized in normal saline were administered *i.p.* 10 min before isoflurane challenge. The 3
169 mg/kg dose did not prevent rise in rectal temperature and only 1 out of 6 mice survived (**Fig.**
170 **4a-4c**). Time to death for mice treated at 3 mg/kg (47±15 min, n=5) was not significantly
171 different than that for control mice (53±24 min, n=9). However, with the 10 mg/kg dose, Cpd1
172 successfully prevented any rise in rectal temperature (**Fig. 4a, 4b**). All the treated mice survived
173 90 min after induction of anesthesia (**Fig. 4c**) and they behaved normally for at least 24 h after
174 recovery from anesthesia.
175 We next tested whether Cpd1 could rescue mice from MH episodes. R2509C mice

176 (both males and females) were anesthetized with isoflurane and the drug was administered *i.p.*
177 when rectal temperature reached 39°C. The 3 mg/kg dose was able to reduce rectal temperature
178 by -0.03±0.81°C at 10 min after administration, compared to an increase of 1.79±0.82°C in
179 controls, but rectal temperature started to rise again ~30 min after administration of the drug in
180 some mice (**Fig. 4d, 4e**). The 10 mg/kg dose decreased body temperature by -0.64±0.29°C at
181 10 min after administration and maintained it at that level until the experiment was terminated
182 60 min after administration of the drug. At that time 60% of the mice in the 3 mg/kg group and
183 100% of the mice in the 10 mg/kg group survived (**Fig. 4f**) and all the survivors behaved
184 normally for at least 24 h after experiments.
185
186 **Effect of Cpd1 on *in vivo* environmental heat stress challenge**
187 It has been shown that environmental heat stress causes an increase in body
188 temperature and death in other MH model mice [29, 30, 33, 34]. We therefore tested whether R2509C
189 mice exhibit heat stroke triggered by environmental heat stress. Mice were anesthetized using
190 intravenous anesthetics and transferred to a 35 °C test chamber. Whereas the rectal temperature
191 of WT mice was maintained at a relatively constant level around 37°C (37.4±0.8°C, n=7), the
192 rectal temperature of R2509C mice steadily increased to 41.4±1.4°C (n=13) (**Supplementary**
193 **Fig. 3a**). Almost all the mice responded to heat and died (**Supplementary Fig. 3b**). Although
194 the time from start of heat stress to death largely varied substantially among individual mice,
195 the variation in time to death after reaching body temperatures of 38°C (36±13 min, n=13) or
196 39°C (22±8 min, n=12) became smaller (**Supplementary Fig. 3c**).
197 Using this model, we initially tested the preventive effect of Cpd1 on the heat stroke.
198 Pretreatment of mice with Cpd1 (10 mg/kg) slowed the rate of temperature rise (**Fig. 5a**), but
199 maximum rectal temperature did not change (**Fig. 5b**) and none of the treated mice (0 out of 4)
200 survived 120 min of heat stress (**Fig. 5c**). However, time to death for the treated mice (98±17

201 min, n=4) was significantly prolonged compared to the control mice (74±21 min, n=13) (**Fig.**
202 **5d**).
203 We next tested whether Cpd1 could rescue mice from environmental heat stroke. The
204 R2509C mice were incubated in the test chamber and the drug was administered *i.p.* when their
205 rectal temperature reached 39°C. All the untreated mice died within 30 min of the time of
206 injection (time to death, 22±8 min, n=13). The 3 mg/kg Cpd1 dose slowed rise in the body
207 temperature post injection (**Fig. 5e, 5f**) and 3 out of 5 mice survived 60 min after administration
208 (**Fig. 5g**). The 10 mg/kg Cpd1 dose showed more pronounced effect: it suppressed rise in the
209 body temperature and 10 out of 11 mice survived for 60 min after administration. After
210 removing from the heat stress environment, the survivors behaved normally for at least 24 h
211 after being and regaining consciousness. When the drug was administered at body temperature
212 of 38°C, after which most untreated mice died within 60 min (time to death, 36±13 min, n=13),
213 both the 3 and 10 mg/kg Cpd1 doses strongly suppressed the continued rise in the body
214 temperature (**Supplementary Fig. 4a, 4b**) and almost all mice survived 60 min after its
215 administration (**Supplementary Fig. 4c**).
216
217 **Pharmacokinetics of Cpd1**
218 We observed transient effects with the 3mg/kg dose of Cpd1 in rescue experiments in both *in*
219 *vivo* isoflurane and heat stress challenges with R2509C mice (see **Fig. 4d, 5e**). This implies fast
220 metabolism or excretion of the drug in mice. We therefore measured plasma concentration of
221 Cpd1 after *i.p.* administration. Cpd1 rapidly declined in mouse blood following first order
222 kinetics with $t_{1/2}$ of ~8 min for both the 3 mg/kg and 10 mg/kg dose (**Fig. 6a**). There was no sex
223 difference in the kinetics of Cpd1 (**Supplementary Fig. 5a, 5b**). Since Cpd1 has hydrophobic
224 moiety of octyl group (see **Fig. 2**), it can be metabolized in the liver. *In vitro* drug metabolism
225 assay using mouse liver microsomes demonstrated that Cpd1 was reduced to 20% and 5% of

226 the original amount at 10 min and 60 min, respectively (**Fig. 6b**). Cpd1 was metabolized more
227 slowly by human liver microsomes; it was reduced to 20% at 60 min.

228 The duration of the effect of Cpd1 in mice was also evaluated using measurements of
229 *in vivo* muscle strength, since we showed that the drug inhibited twitch and tetanic contractions
230 in isolated skeletal muscle (see **Fig. 2**). Grip strength tests demonstrated that muscle strength
231 of WT mice was reduced by 15% 10 min after administration of 10 mg/kg Cpd1, and that this
232 deficit was almost completely recovered at 60 min, suggesting short duration of the medicinal
233 effect *in vivo* (**Fig. 6c**). No sex nor genotype differences were observed in the effect of Cpd1
234 on *in vivo* muscle contraction strength (**Supplementary Fig. 6a-6c**).

235 The above results indicate that transient effects of Cpd1 in the isoflurane challenge
236 and heat challenge experiments are due to rapid metabolism of the drug in mice. In fact, second
237 and third administrations of the 3 mg/kg dose when rectal temperature reached 39°C
238 successfully decreased the rectal temperature (**Supplementary Fig. 7**). We therefore tested
239 whether repeated administrations of Cpd1 could prevent mice from the crisis. Eight
240 administrations of 1 mg/kg Cpd1 at 10 min intervals successfully prevented rise in the rectal
241 temperature by exposure either to isoflurane (**Fig. 6d**) or to heat stress (**Fig. 6e**) and all the mice
242 survived the full 90 min after initiating either challenge (**Fig. 6f**). Pharmacokinetic analysis of
243 Cpd1 after repeated administrations revealed that Cpd1 rapidly declined from mouse blood as
244 was case of single administration (**Fig. 6g**). Interestingly, $t_{1/2}$ was slightly longer in female
245 (14.8±2.1 min, n=3) than in male (9.6±2.7 min, n=3), whereas C_{max} was significantly higher in
246 males (0.67±0.11 μg/mL, n=3) than in females (0.15±0.11 μg/mL, n=3). Muscle weakness was
247 transiently observed after the repeated administrations in both male and female, but it returned
248 to normal by 60 min (**Fig. 6h**).

249

250 **Effect of Cpd1 on RYR1-p.R163C MH model mice**

251 We demonstrated that Cpd1 prevented and reversed MH and heat stroke in R2509C mice. To
252 test whether this is also the case with other MH model mice carrying different mutations, we
253 examined the effects of Cpd1 on heterozygous *RYR1*-p.R163C (R163C) mice [29] using *in vivo*
254 measurements of $[Ca^{2+}]_i$ with Ca^{2+}-selective microelectrodes [38]. Resting $[Ca^{2+}]_i$ was threefold
255 higher in R163C muscle (330 ± 43 nM, n = 17) compared to WT muscle (122 ± 3 nM, n = 20)
256 (**Fig. 7a**). Administration of Cpd1 *i.p.* effectively reduced $[Ca^{2+}]_i$ in R163C muscle in a dose-
257 dependent manner. Cpd1 also reduced $[Ca^{2+}]_i$ in WT muscles, but the effect was significantly
258 smaller. When mice were exposed to 1.5% (v/v) isoflurane, $[Ca^{2+}]_i$ rapidly increased in
259 untreated R163C muscles (1226 ± 154 nM, n = 19), indicating a MH episode (**Fig. 7b, 7c**).
260 Administration of isoflurane had no effect on $[Ca^{2+}]_i$ in WT muscles (121 ± 4 nM, n = 18) (**Fig.
261 7c**). Pretreatment with Cpd1 suppressed increase in $[Ca^{2+}]_i$ in R163C muscle in a dose-
262 dependent manner (**Fig. 7b, 7c**) and effectively prevented the MH episode and death at doses
263 of 5 and 10 mg/kg (**Fig. 7d**). When Cpd1 at 10 mg/kg was administered to R163C mice 15 min
264 after induction of isoflurane anesthesia, it was able to abort the MH crisis and rapidly decreased
265 $[Ca^{2+}]_i$ to the levels measured in WT muscle (**Fig. 7e, 7f**).
266 To validate *in vivo* experiments, we tested the effect of Cpd1 in FDB muscle fibers
267 isolated from the R163C mice. Similar to the *in vivo* findings, $[Ca^{2+}]_i$ was significantly higher
268 in quiescent R163C fibers (326 ± 27 nM, n = 16) compared to WT fibers (121 ± 3 nM, n = 20)
269 and Cpd1 reduced $[Ca^{2+}]_i$ in R163C fibers in a dose-dependent manner to the level of WT fibers.
270 (**Supplementary Fig. 8**).
271
272 **Effect of Cpd1 on RYR1-p.G2435R MH model mice**
273 We also tested the effect of Cpd1 on a third MH model using homozygous *RYR1*-p.G2435R
274 mice [30]. The G2435R mice exhibit severe heat stroke by environmental heat stress. When
275 unanesthetized restrained G2435R mice were exposed to an ambient temperature of 38° C,

276 their rectal temperature rapidly increased and reached 40°C within 20 min (the experiment was
277 terminated at this point) (**Fig. 8a**). Pretreatment of G2435R mice with Cpd1 (30 mg/kg) greatly
278 slowed the rise in rectal temperature (**Fig. 8b**).

279 *RYR1*-p.G2435R muscles have also been shown to have enhanced cation influx
280 compared to WT which is thought to be in response to chronic reduced SR Ca^{2+} load [30]. To test
281 the effect of Cpd1 on sarcolemmal cation influx, we measured resting Mn^{2+} quench of fura-2
282 fluorescence in isolated G2435R and WT skeletal muscle fibers. The rate of Mn^{2+} quench in
283 G2435R fibers was twice that in WT fibers (**Fig. 8c, 8d**). Cpd1 reduced Mn^{2+} quench in G2435R
284 fibers in a dose-dependent manner and the Mn^{2+} quench rate at the 10 μM dose was the same
285 as untreated WT fibers.

286

287 **Discussion**

288 Here we examined the therapeutic effects of Cpd1, a novel RyR1-selective inhibitor
289 with high potency [26], on the volatile anesthetic and increased environmental temperature-
290 induced MH crisis. Cpd1 showed good solubility in normal saline (Table 1). Using three
291 different model mice, we demonstrated that Cpd1: (1) prevents increase in $[Ca^{2+}]_i$ by volatile
292 anesthetics (halothane and isoflurane) and decreases resting $[Ca^{2+}]_i$ in skeletal muscle *in vitro*
293 and *in vivo* (**Figs. 2, 7**), (2) inhibits sarcolemmal cation entry caused by chronic store Ca^{2+}
294 depletion (**Fig. 8**), (3) inhibits caffeine- and heat-induced contracture in isolated skeletal
295 muscle (**Fig. 3**), (4) effectively prevents and treats isoflurane-induced fulminant MH crisis
296 (**Figs. 4, 7**), and (5) treats severe heat stroke caused by environmental heat stress (**Figs. 5, 8**).
297 These results provide crucial evidence that Cpd1 is capable of effectively preventing and
298 treating the MH crisis and heat stroke by inhibiting the RyR1 channel.

299 Several strains of MH mouse models carrying mutations in the *RYR1* gene have
300 been reported to date [29, 30, 33, 34]. We created a novel mouse model carrying p.R2509C mutation

301 in the *RYR1* gene, which corresponds to MH mutation (p.R2508C) in human *RYR1* gene [27]. In
302 a HEK293 expression system, the p.R2508C mutant exhibited the highest CICR activity
303 among mutants in the central region tested [28].Whereas homozygous mice were embryonic
304 lethal, heterozygous mice grew normally and were as fertile as WT (**Fig. 1**). R2509C mice
305 showed a halothane- and isoflurane-induced increase in $[Ca^{2+}]_i$ (**Fig. 2**) and caffeine- and
306 heat-induced contracture in skeletal muscle (**Fig. 3**). In addition, they exhibited a MH crisis
307 when exposed to isoflurane anesthesia (**Fig. 1**) and heat stroke when exposed to
308 environmental heat stress (**Fig. 5, Supplementary Fig. 3**). These properties are common to
309 those seen in the other model mice carrying severe MH mutations in the *RYR1* gene, e.g.,
310 p.R163C [29] and p.Y524S [33]. Thus, R2509C mice are a useful model for MH research.
311 Interestingly, time to death by isoflurane anesthesia of R2509C mice (64±30 min, **Fig. 1**) was
312 much longer than that of R163C mice (<20 min, **Fig. 7**). Correspondingly, increase in resting
313 $[Ca^{2+}]_i$ appeared smaller in R2509C muscle (**Fig. 2**) than in R163C muscle (**Fig. 7**,
314 **Supplementary Fig. 8**). These findings suggest that R2509C mice show milder phenotype
315 than R163C mice.
316 Although dantrolene is the only compound that is available and used to treat and
317 prevent MH, a major problem of dantrolene in clinical use is its poor aqueous solubility [22].
318 First, dantrolene must be solubilized with sterile water and injected or infused by the
319 intravenous route, since it is virtually insoluble in normal saline. Second, dantrolene is
320 prepared at a diluted concentration (0.33 mg/mL) due to its low water solubility, which makes
321 rapid preparation difficult in emergency situations. Whereas the second problem has recently
322 been solved by nanocrystalline suspension of dantrolene (Ryanodex®) which can be injected
323 at a concentration of 50 mg/mL [43], the first problem remains unsolved to date. We found that
324 Cpd1 exhibits good solubility (849±58 μg/mL) in normal saline, which is 34-fold higher
325 compared to dantrolene (25.7±2.1 μg/mL) (**Table 1**). This enables continuous administration

326 of the drug by infusion using the intravenous route and expands usage of the drug before and
327 after surgery for prevention of MH and postoperative MH [44].
328 Another drawback of dantrolene in clinical use is its long plasma half-life (10-12 h
329 in humans after intravenous injection) [45]. Therefore, it is difficult to control the appropriate
330 plasma concentration and reduce side effects such as muscle weakness [22]. Pharmacokinetic
331 analysis revealed that Cpd1 is rapidly metabolized in mice with plasma half-life of ~8 min,
332 probably by metabolism by the liver (**Fig. 6**). Muscle weakness was completely recovered
333 within 60 min (**Fig. 6**). Rapid metabolism of Cpd1 was also true even after repeated
334 administration of 1 mg/kg Cpd1 at 10 min intervals, which successfully prevented rise in the
335 rectal temperature by exposure either to isoflurane or heat stress (**Fig. 6**). Thus, Cpd1 may be
336 beneficial for a treatment of MH episodes without the concern of residual weakness.
337 Heat stroke is a life-threatening condition clinically diagnosed as a severe elevation
338 in body temperature with central nervous system dysfunction [12, 13]. It has been reported that
339 MH mutations in the *RYR1* gene is implicated in some heat stroke [14, 15, 16]. Dantrolene has
340 therapeutic effects on some patients with severe exertional heat stroke [46]. Cpd1 effectively
341 prevents and treats fulminant heat stroke caused by environmental heat stress in both R2509C
342 (**Figs. 5, 6**) and G2435R (**Fig. 8**) model mice. Since Cpd1 is soluble in normal saline, it has
343 the potential to be administered by continuous infusion which could be necessary for
344 treatment of severe heat stroke without the concern for prolonged muscle weakness.
345 Dantrolene is also used for the treatment of neuroleptic malignant syndrome, a life-
346 threatening neurologic emergency associated with the use of antipsychotic agents [47] as well as
347 overdose of 2,4-dinitrophenol (a prohibited weight loss agent that interrupts ATP synthesis
348 and causes hyperthermia) [48]. Since Cpd1 has similar effects in preventing and treating MH
349 and heat stroke, it might also be a potential candidate for treatment of these emergency
350 situations.

351

352 **Materials and Methods**

353

354 **Materials**

355 Cpd1 was synthesized as described previously [26]. Sodium salt of Cpd1 was prepared as
356 follows. Cpd1 (100 mg, 0.29 mmol) was dissolved in 3 mL of tetrahydrofuran. Then, 44 μL
357 of NaOH aqueous solution (25%, 0.28 mmol) was added to the solution, and the suspension
358 was sonicated for 10 min to afford white precipitate. After 24 h at room temperature, the
359 colorless precipitates were collected by filtration, and washed with cold tetrahydrofuran. The
360 residual material was dried under reduced pressure to give the sodium salt of Cpd1 as
361 colorless powder.

362

363 **Determination of thermodynamic solubility**

364 Test compound (2 mg) was suspended with 1 mL of normal saline, pure water, or 5% glucose
365 aqueous solution in glass tube, and the suspension was shaken at 150 rpm for 48 h at 25 °C.
366 An aliquot was filtered by PVDF filter unit (Mini-Uni Prep™, GE Healthcare), and the
367 filtrate was diluted with pure water. The diluted sample solution was injected into HPLC
368 system (column (Mightysil RP-18, Kanto Chemical Co. Inc.), UV/vis detector (UV-2077,
369 JASCO), pump (PU-2089, JASCO), and column oven (CO-965, JASCO)) and the peak area
370 was recorded at 254 nm. The concentration of solution was calculated with a calibration
371 curve. Examinations of all conditions were performed three or four times.

372

373 **Animals**

374 All animal-related procedures were in accordance with the guidelines of the Jikei University
375 School of Medicine, Juntendo University School of Medicine, the National Center of

376 Neurology and Psychiatry (NCNP), Mount Sinai Hospital and UK Home Office, administered
377 by the University of Leeds. Mice were housed in isolator cages, fed with food and water ad
378 libitum, and kept under controlled lighting conditions (12 h-light/12 h-dark) in specific
379 pathogen-free conditions in the Jikei University, Juntendo University, National Institute of
380 Neuroscience, NCNP, Mount Sinai Hospital and the Leeds Institute of Medicine animal
381 facilities.
382
383 **Generation of mutant mouse by gene editing using CRISPR-Cas9 system**
384 Mouse genomic sequence within upstream- and downstream-50 bps each to that
385 corresponding to human mutation site was searched by CRISPR design tool
386 (http://crispr.mit/edu) to select PAM and its consequent guide sequence with high specificity.
387 CAATGCCATACACTCGGTCC**AGG** (bold: PAM sequence) was selected for crRNA
388 synthesis. A single-stranded donor oligonucleotide carrying *Xba* I site (underlined),
389 CCGAAGATGTCTGCATCCTTCGTGCCTGACCAGGCATCCATGGTGCTTTTTCTAGA
390 CTGCGTGTATGGCATTGAGAACCAGGACTTCTTGCTGCATGTGCTGGATGTGGG
391 was chemically synthesized for homologous recombination (**Fig. 1**). A *RYR1*-genomic
392 fragment containing PAM and the consequent guide sequence were amplified by PCR from
393 wild-type mouse genomic DNA. RNP complex formed by mixing of tracrRNA and crRNA
394 with recombinant Cas9 protein, was added to the PCR fragment and incubated for 1 hour.
395 Cleavage of PCR fragment into two fragments was confirmed by agarose electrophoresis.
396 RNP complex and single-stranded donor oligonucleotide were introduced to mouse one-cell-
397 stage zygotes by electroporation. The electroporated zygotes were transferred to the oviducts
398 of pseudopregnant females. Genomic DNA was prepared from newborns' tail and knock-in
399 mice were screened by PCR-RFLP method using a pair of primers (R2509C_Forward:
400 GCGTCAGGAATGGTTAGAATAGAT; R2509C_Reverse:

401 TTGTCTGATGCTAGGTAGAAGGTG) and *Xba* I digestion (**Fig. 1**). Crossing obtained
402 knock-in founders with wild-type mice to get F1 generations were done by standard protocol.
403
404 **Preparation of single flexor digitorum brevis (FDB) cells**
405 WT and mutant mice (R2509C, 8- to 20-week old; R163C, 12- to 16-week old, and G2435R,
406 12- to 16-week old) were euthanized and flexor digitorum brevis (FDB) muscles were
407 dissected and incubated with 2 mg/mL collagenase (Worthington Biochemical Co., NJ, USA)
408 in the HEPES-Krebs solution containing 2 mg/mL bovine serum albumin for 2-3 hours at
409 37°C. Following incubation, single cells were separated by gentle trituration in collagenase-
410 free HEPES-Krebs solution. Isolated single FDB cells were seeded on a laminin-coated cover
411 slip of the 35 mm glass-bottom dish or on 96 well plate coated with Cultrex basement
412 membrane matrix (Trevigen, Minneapolis, USA).
413
414 **Ca^{2+} imaging of isolated single FDB cells**
415 Isolated single FDB cells were incubated with 4 μM Cal520-AM (AAT Bioquest, CA, USA)
416 or fura-2-AM (Thermo Fisher Scientific) dye in the HEPES-Krebs solution (140 mM NaCl, 5
417 mM KCl, 2 mM $CaCl_2$, 1 mM $MgCl_2$, 11 mM glucose, 5 mM HEPES, pH 7.4) for 30 min at
418 37°C. The cells were then washed three times with the HEPES-Krebs solution to remove
419 excess dye, and after 30 min of de-esterification, fluorescence images were obtained with a
420 20X (NA=0.75) objective lens of an inverted microscope (Nikon TE2000-E Japan) equipped
421 with the sCMOS camera (Zyla, Andor, Belfast, Northern Ireland). Cal520 was excited at
422 480±15 nm, and fluorescence was measured at wavelengths of 525±25 nm. Fura-2 was
423 excited at alternating lights of 340±6 nm and 380±6 nm, fluorescent light was detected at
424 510±40 nm, and the ratio of fluorescence excited at 340 nm to that at 380 nm was determined.
425 Imaging experiments were carried out at 26°C by superfusing a HEPES-Krebs solution with

426 or without halothane or isoflurane. Cpd1 was administered 5 min before measurements. For
427 Mn^{2+} quenching experiments, fura-2 was excited at 360±12 nm and emitted fluorescence at
428 510±40 nm was monitored. The cells were perfused with basal Krebs solution (140 mM
429 NaCl, 5 mM KCl, 1 mM $MgCl_2$, 11 mM glucose, 2 mM $CaCl_2$, 10 mM HEPES, pH 7.4) for
430 60 sec to obtain the baseline signal and then perfused with Mn^{2+} quenching Krebs solution
431 (140 mM NaCl, 5 mM KCl, 1 mM $MgCl_2$, 11 mM glucose, 0.5 mM $MnCl_2$, 10 mM HEPES,
432 pH 7.4) for 180 s followed by reperfusion with basal Krebs solution for 120 sec.
433
434 **Measurement of muscle force *in vitro***
435 Muscle contraction measurement was assessed using intact soleus muscle as described
436 previously [49]. WT and R2509C mice (8- to 20-week old) were anesthetized with an *i.p.*
437 injection of sodium pentobarbital (70 mg/kg body weight) and the soleus muscles were
438 dissected. The isolated muscles were mounted between a force transducer (UL-100; Minebea
439 Co., Tokyo, Japan) and a fixed hook in a chamber containing Krebs solution (140 mmol/L
440 NaCl, 5 mmol/L KCl, 2 mmol/L $CaCl_2$, 1 mmol/L $MgCl_2$, 1 mmol/L NaH_2PO_4, 25 mmol/L
441 $NaHCO_3$, and 11 mmol/L glucose) bubbled with 95% O_2 and 5% CO_2 at 25°C. The muscles
442 were stretched to determine the length which produced maximum twitch contraction in
443 response to field stimulation for 1 msec at supramaximal voltage. For caffeine contracture
444 studies, muscles were exposed for 2 min to Krebs solution containing 10, 15, or 20 mM
445 caffeine. For heat-induced contracture studies, muscles were exposed to Krebs solution
446 warmed at 27, 35, 40 and 42°C until basal force peaked. For twitch and tetanic contraction
447 measurements, muscles were stimulated at 1 min intervals with 20 trains of 1, 2, 5, 10, 20, 50,
448 100, and 200 Hz pulses. For Cpd1 treatment, muscles were incubated with Krebs solution
449 containing 3 μM Cpd1 15 min prior to measurements. Absolute contractile force was
450 normalized to the maximum diameter of the muscle.

451

452 ***In vivo* isoflurane challenge**

453 WT and R2509C mice (8- to 20-week old) were weighed and then placed into an anesthetic
454 chamber. Anesthesia was induced with 2.0-3.0 vol% isoflurane in air using a precision
455 vaporizer (TK-7w BioMachinery isoflurane system, Japan) until there was no detectable
456 response to tweezer pinches (within 60 s). Then, mice were rapidly placed atop a bed
457 prewarmed at 37°C and anesthesia was maintained with isoflurane, 1.5-2.0 vol% in air via a
458 nose cone attachment. Rectal temperature was continuously monitored with a rectal probe
459 (RET-3; Physitemp Instruments, LLC, NJ, USA) using Powerlab 26T (AdInstruments,
460 Dunedin, New Zealand). Data were recorded every 10 s for up to 90 min or until the animal
461 died of an MH crisis. Cpd1 was administered *i.p*. either 10 min before the start of isoflurane
462 anesthesia for test of the preventive effect or when the rectal temperature was achieved 39°C
463 for treatment of MH episodes.

464

465 ***In vivo* heat stress challenge**

466 **In anesthetized R2509C mice.** To investigate heat stress responses, WT and R2509C mice
467 (8- to 20-week old) were anesthetized *i.p*. with an anesthetic mixture (0.75 mg/kg
468 medetomidine, 4 mg/kg midazolam and 5 mg/kg butorphanol) and transferred to a test
469 chamber prewarmed at 35°C. Rectal temperature was measured continuously during the heat
470 stress challenge (up to 120 min) or until death of animals by fulminant heat stroke. Cpd1 was
471 administered *i.p*. either 10 min before the start of heat stress challenge for test of the
472 preventive effect or when the rectal temperature was achieved at 38 or 39°C for treatment of
473 heat stroke.

474 **In awake restrained G2435R mice**. In this model to investigate the heat stress response,
475 G2435R mice (12- to 16-week old) was administered Cpd1 *i.p.*, placed into a mouse restrainer

476 (Kent Scientific, CT, USA), and placed in an environmental chamber warmed to 38°C. Rectal
477 temperature was monitored continuously with a probe and recorded every min. When the
478 rectal temperature reached 40°C the experiment was ended and the animal was euthanized by
479 cervical dislocation.
480
481 **Ca^{2+} determinations in intact muscle fibers using ion-specific microelectrodes**
482 Ca^{2+} ion specific microelectrode recordings were performed as described previously [38, 50]. For
483 *in vivo* measurements, WT and *RYR1*-p.R163C heterozygous mice (12- to 16-week old) were
484 anesthetized by *i.p.* injection of 100 mg/kg ketamine and 5 mg/kg xylazine and placed on a
485 37°C heating pad and their temperature was monitored. The *vastus lateralis* was exposed
486 surgically after which its muscle fibers were impaled with double-barreled Ca^{2+}-selective
487 microelectrode, and the potentials were recorded via a high-impedance amplifier (WPI Duo
488 773 electrometer; WPI, Sarasota, FL, USA). The potential from the 3 M KCl microelectrode
489 (V_m) was subtracted electronically from the potential of the Ca^{2+} electrode (V_{CaE}) to produce a
490 differential Ca^{2+}-specific potential (V_{Ca}) that represents the $[Ca^{2+}]_i$. V_m and V_{Ca} were filtered
491 (30–50 kHz) to improve the signal-to-noise ratio and stored in a computer for further analysis.
492 Determinations were carried out at resting condition and then 5-10 min after commencing
493 exposure to 1.5% isoflurane in the inspired air. Cpd1 (0-10 mg/kg) was administered *i.p.*
494 before exposure to isoflurane and measurements made every 5 min. For *in vitro*
495 measurements, single flexor digitorum brevis (FDB) muscle fibers were enzymatically
496 isolated as described above and placed in mammalian Ringer solution of following
497 composition (in mM): 140 NaCl, 5 KCl, 2 $CaCl_2$, 1 $MgCl_2$, 5 glucose, and 10 HEPES, pH 7.4.
498 Muscle fibers were impaled with the microelectrodes as above and $[Ca^{2+}]_i$ was determined in
499 the presence of varying (0-5 μM) concentrations of Cpd1.
500

501 **Mn^{2+} quench assay**

502 Assays were carried out as described previously [38]. 5µM of fura2-AM dye (Thermo Fisher
503 Scientific) dissolved in mammalian Ringer solution (133 mM NaCl, 5 mM KCl, 1 mM
504 $MgSO_4$, 25 mM HEPES, 5.5 mM glucose, 2 mM $CaCl_2$, pH 7.4) was loaded onto the
505 dissociated WT and *RYR1*-p.G2435R homozygous FDB fibers in 96 well plates for 30 mins at
506 37°C, 5% CO_2. Fibers were then washed twice with Ringer solution and then incubated with
507 the desired concentration of Cpd1 dissolved in Ringer solution for the final wash in the drug
508 treated samples. After washing fibers were maintained at 37°C for 20 mins for de-
509 esterification of fura2-AM and in the presence of the tested concentration of Cpd1. The fibers
510 were then transferred to the stage of a Nikon TE2000 inverted microscope (Nikon, Tokyo,
511 Japan). Fura-2 was illuminated at its isosbestic wavelength (360nm) with the X-Cite 120
512 metal halide light source (Exfo, Ontario, Canada) and fluorescence emission at 510 nm was
513 recorded using a 10 x 0.3na objective. The fibers were perfused with Ringer solution for 30
514 sec to obtain the baseline signal and then perfused with manganese quench buffer (133 mM
515 NaCl, 5 mM KCl, 0.5 mM $MnCl_2$, 25 mM HEPES, 5.5 mM glucose, pH 7.4) for 180 s
516 followed by reperfusion with Ringer solution for 30 sec to wash away the manganese quench
517 buffer. Data were collected using an intensified 10-bit digital intensified CCD at 30 fps
518 (Stanford Photonics, Stanford, CA) from regions of interest on 3-6 individual fibers per well
519 and analyzed using Piper software (Stanford Photonics, Stanford, CA). The fluorescence
520 signals were plotted as arbitrary fluorescence units over time. GraphPad Prism 7 was used to
521 fit the baseline signal and quench signal into linear regression models ($y = mx + c$). The
522 fluorescence quench rate was calculated by subtracting the slope of the baseline signal from
523 that of the quench signal to obtain the net slope for both drug-treated and untreated samples.
524

525 **Pharmacokinetics**

526 Cpd1 sodium salt (3 mg/kg and 10 mg/kg) dissolved in normal saline was administered *i.p.* to
527 WT C57BL/6J mice (10 week-old). Serial tail bled blood samples (~20 μL) were collected
528 using heparinized tip at 5, 10, 30, and 60 min after administration. Aliquots (5μL) of plasma
529 samples obtained from each blood were treated with 50 μL of acetonitrile and organic layer
530 were injected onto LC-MS/MS system (Waters Corp., Milford, MA, USA). The
531 pharmacokinetic parameters included maximum concentration (C_{max}), elimination half-life ($T_{½}$).
532

533 **Metabolic stability in liver microsomes.**

534 Cpd1 (final concentration was 0.5 μM) was incubated with human or mouse hepatic
535 microsomes (XenoTech Ltd, Kansas City, KS) with nicotinamide adenine dinucleotide
536 phosphate (NADPH) for 10 and 60 min at 37°C. Each reaction was stopped by acetonitrile, and
537 the value of unchanged compound 1 was determined by quantitating using LC-MS/MS, and the
538 metabolic stability was evaluated as a remaining rate (%).
539

540 **Measurement of muscle force *in vivo***

541 Muscle force was measured *in vivo* by grip-force test. The tests were performed as blinded, so
542 the experimenter did not know which kind of solution (vehicle or Cpd1) was injected to each
543 mouse. The force was measured before and 10 and 60 min after *i.p.* injection of saline or
544 Cpd1 (10 mg/kg). Mice (8- to 12-week old) were gently held by the tails and allowed them to
545 grasp the horizontally positioned metal bar of the Grip Strength Meter (MK308M,
546 Muromachi Kikai, Tokyo, Japan) with their forelimbs and hindlimbs (4-grips test). Each
547 mouse performed four trials for force measurement at every time point. The highest force
548 value applied to the metal bar was recorded and normalized by body weight [51].
549

550 **Statistics**

551 Data are presented as the mean ± SD. Statistical analysis was performed using Prism 8
552 (GraphPad Software, Inc., La Jolla, USA). Student's *t*-test was used for comparisons between
553 two groups. One-way analysis of variance (ANOVA), followed by Dunnett's test, was
554 performed to compare multiple groups. Statistical significance was defined as $p < 0.05$.
555

556 **References**

557 1. Meissner G. Ryanodine receptor/Ca^{2+} release channels and their regulation by
558 endogenous effectors. Annu Rev Physiol 56, 485-508 (1994).
559 2. Ogawa Y. Role of ryanodine receptors. Crit Rev Biochem Mol Biol 29, 229-274 (1994).
560 3. Rios E, Pizarro G, Stefani E. Charge movement and the nature of signal transduction in
561 skeletal muscle excitation-contraction coupling. Annu Rev Physiol 54, 109-133 (1992).
562 4. Schneider MF. Control of calcium release in functioning skeletal muscle fibers. Annu
563 Rev Physiol 56, 463-484 (1994).
564 5. Endo M. Calcium release from the sarcoplasmic reticulum. Physiol Rev 57, 71-108
565 (1977).
566 6. Endo M. Calcium-induced calcium release in skeletal muscle. Physiol Rev 89, 1153-
567 1176 (2009).
568 7. Murayama T, Kurebayashi N. Two ryanodine receptor isoforms in nonmammalian
569 vertebrate skeletal muscle: possible roles in excitation-contraction coupling and other
570 processes. Prog Biophys Mol Biol 105, 134-144 (2011).
571 8. Robinson R, Carpenter D, Shaw MA, Halsall J, Hopkins P. Mutations in RYR1 in
572 malignant hyperthermia and central core disease. Hum Mutat 27, 977-989 (2006).
573 9. Hopkins PM. Malignant hyperthermia: advances in clinical management and diagnosis.
574 Br J Anaesth 85, 118-128 (2000).
575 10. Loke J, MacLennan DH. Malignant hyperthermia and central core disease: disorders of
576 Ca^{2+} release channels. Am J Med 104, 470-486 (1998).
577 11. Mickelson JR, Louis CF. Malignant hyperthermia: excitation-contraction coupling, Ca^{2+}
578 release channel, and cell Ca^{2+} regulation defects. Physiol Rev 76, 537-592 (1996).
579 12. Leon LR, Bouchama A. Heat stroke. Compr Physiol 5, 611-647 (2015).
580 13. Hifumi T, Kondo Y, Shimizu K, Miyake Y. Heat stroke. J Intensive Care 6, 30 (2018).
581 14. Davis M, *et al.* Malignant hyperthermia associated with exercise-induced
582 rhabdomyolysis or congenital abnormalities and a novel RYR1 mutation in New

583 Zealand and Australian pedigrees. Br J Anaesth 88, 508-515 (2002).
584 15. Wappler F, *et al.* Evidence for susceptibility to malignant hyperthermia in patients with
585 exercise-induced rhabdomyolysis. Anesthesiology 94, 95-100 (2001).
586 16. Tobin JR, Jason DR, Challa VR, Nelson TE, Sambuughin N. Malignant hyperthermia
587 and apparent heat stroke. JAMA 286, 168-169 (2001).
588 17. Kolb ME, Horne ML, Martz R. Dantrolene in human malignant hyperthermia.
589 Anesthesiology 56, 254-262 (1982).
590 18. Krarup C. The effect of dantrolene on the enhancement and diminution of tension
591 evoked by staircase and by tetanus in rat muscle. J Physiol 311, 389-400 (1981).
592 19. Snyder HR, Jr., Davis CS, Bickerton RK, Halliday RP. 1-[(5-
593 arylfurfurylidene)amino]hydantoins. A new class of muscle relaxants. J Med Chem 10,
594 807-810 (1967).
595 20. Paul-Pletzer K, Palnitkar SS, Jimenez LS, Morimoto H, Parness J. The skeletal muscle
596 ryanodine receptor identified as a molecular target of [3H]azidodantrolene by
597 photoaffinity labeling. Biochemistry 40, 531-542 (2001).
598 21. Zhao F, Li P, Chen SR, Louis CF, Fruen BR, Mickelson JR. Dantrolene inhibition of
599 ryanodine receptor Ca^{2+} release channels. Molecular mechanism and isoform selectivity.
600 J Biol Chem 276, 13810-13816 (2001).
601 22. Krause T, Gerbershagen MU, Fiege M, Weisshorn R, Wappler F. Dantrolene: a review
602 of its pharmacology, therapeutic use and new developments. Anaesthesia 59, 364-373
603 (2004).
604 23. Flewellen EH, Nelson TE, Jones WP, Arens JF, Wagner DL. Dantrolene dose response
605 in awake man: implications for management of malignant hyperthermia.
606 Anesthesiology 59, 275-280 (1983).
607 24. Murayama T, Kurebayashi N. Assays for Modulators of Ryanodine Receptor
608 (RyR)/Ca($^{2+}$) Release Channel Activity for Drug Discovery for Skeletal Muscle and
609 Heart Diseases. Curr Protoc Pharmacol 87, e71 (2019).
610 25. Murayama T, *et al.* Efficient high-throughput screening by endoplasmic reticulum Ca^{2+}
611 measurement to identify inhibitors of ryanodine receptor Ca^{2+}-release channels. Mol
612 Pharmacol 94, 722-730 (2018).
613 26. Mori S, *et al.* Structural development of a type-1 ryanodine receptor (RyR1) Ca^{2+}-
614 release channel inhibitor guided by endoplasmic reticulum Ca^{2+} assay. Eur J Med Chem
615 179, 837-848 (2019).
616 27. Ibarra MC, *et al.* Malignant hyperthermia in Japan: mutation screening of the entire
617 ryanodine receptor type 1 gene coding region by direct sequencing. Anesthesiology 104,

618 1146-1154 (2006).
619 28. Murayama T, *et al.* Genotype-phenotype correlations of malignant hyperthermia and
620 central core disease mutations in the central region of the RYR1 channel. Hum Mutat
621 37, 1231-1241 (2016).
622 29. Yang T, *et al.* Pharmacologic and functional characterization of malignant hyperthermia
623 in the R163C RyR1 knock-in mouse. Anesthesiology 105, 1164-1175 (2006).
624 30. Lopez JR, Kaura V, Diggle CP, Hopkins PM, Allen PD. Malignant hyperthermia,
625 environmental heat stress, and intracellular calcium dysregulation in a mouse model
626 expressing the p.G2435R variant of RYR1. Br J Anaesth 121, 953-961 (2018).
627 31. Allen PD, Lopez JR, Sanchez V, Ryan JF, Sreter FA. EU 4093 decreases intracellular
628 [Ca^{2+}] in skeletal muscle fibers from control and malignant hyperthermia-susceptible
629 swine. Anesthesiology 76, 132-138 (1992).
630 32. Lopez JR, Allen PD, Alamo L, Jones D, Sreter FA. Myoplasmic free [Ca^{2+}] during a
631 malignant hyperthermia episode in swine. Muscle Nerve 11, 82-88 (1988).
632 33. Chelu MG, *et al.* Heat- and anesthesia-induced malignant hyperthermia in an RyR1
633 knock-in mouse. FASEB journal : official publication of the Federation of American
634 Societies for Experimental Biology 20, 329-330 (2006).
635 34. Yuen B, *et al.* Mice expressing T4826I-RYR1 are viable but exhibit sex- and genotype-
636 dependent susceptibility to malignant hyperthermia and muscle damage. FASEB
637 journal : official publication of the Federation of American Societies for Experimental
638 Biology 26, 1311-1322 (2012).
639 35. Jansen ACA, Hilbers HW, Ni XR, Helden SPv, Janssen LHM. Some physical-chemical
640 properties of dantrolene and two of its analogues. Int J Pharm 75, 193-199 (1991).
641 36. Lopez JR, Gerardi A, Lopez MJ, Allen PD. Effects of dantrolene on myoplasmic free
642 [Ca^{2+}] measured in vivo in patients susceptible to malignant hyperthermia.
643 Anesthesiology 76, 711-719 (1992).
644 37. Hopkins PM. Malignant hyperthermia: pharmacology of triggering. Br J Anaesth 107,
645 48-56 (2011).
646 38. Eltit JM, Ding X, Pessah IN, Allen PD, Lopez JR. Nonspecific sarcolemmal cation
647 channels are critical for the pathogenesis of malignant hyperthermia. FASEB journal :
648 official publication of the Federation of American Societies for Experimental Biology
649 27, 991-1000 (2013).
650 39. Yarotskyy V, Protasi F, Dirksen RT. Accelerated activation of SOCE current in
651 myotubes from two mouse models of anesthetic- and heat-induced sudden death. PLoS
652 One 8, e77633 (2013).

653 40. Larach MG. Standardization of the caffeine halothane muscle contracture test. North
654 American Malignant Hyperthermia Group. Anesth Analg 69, 511-515 (1989).
655 41. Leslie GC, Part NJ. The action of dantrolene sodium on rat fast and slow muscle in vivo.
656 Br J Pharmacol 72, 665-672 (1981).
657 42. Meyler WJ, Mols-Thurkow I, Scaf AH, Sargo S, Wesseling H. The effect of dantrolene
658 sodium on rat skeletal muscle in relation to the plasma concentration. Eur J Pharmacol
659 53, 335-342 (1979).
660 43. Schutte JK*, et al.* Comparison of the therapeutic effectiveness of a dantrolene sodium
661 solution and a novel nanocrystalline suspension of dantrolene sodium in malignant
662 hyperthermia normal and susceptible pigs. Eur J Anaesthesiol 28, 256-264 (2011).
663 44. Sinha AK, Kumari P, Vaghela MM, Sinha C, Kumar B. Postoperative Malignant
664 Hyperthermia- A Medical Emergency: A Case Report and Review of Literature. J Clin
665 Diagn Res 11, PD01-PD02 (2017).
666 45. Lerman J, McLeod ME, Strong HA. Pharmacokinetics of intravenous dantrolene in
667 children. Anesthesiology 70, 625-629 (1989).
668 46. Hadad E, Cohen-Sivan Y, Heled Y, Epstein Y. Clinical review: Treatment of heat stroke:
669 should dantrolene be considered? Crit Care 9, 86-91 (2005).
670 47. Simon LV, Hashmi MF, Callahan AL. Neuroleptic Malignant Syndrome. In: StatPearls)
671 (2020).
672 48. Grundlingh J, Dargan PI, El-Zanfaly M, Wood DM. 2,4-dinitrophenol (DNP): a weight
673 loss agent with significant acute toxicity and risk of death. J Med Toxicol 7, 205-212
674 (2011).
675 49. Eshima H*, et al.* Long-term, but not short-term high-fat diet induces fiber composition
676 changes and impaired contractile force in mouse fast-twitch skeletal muscle. Physiol
677 Rep 5, e13250 (2017).
678 50. Lopez JR, Alamo L, Caputo C, DiPolo R, Vergara S. Determination of ionic calcium in
679 frog skeletal muscle fibers. Biophys J 43, 1-4 (1983).
680 51. Anderson KD, Abdul M, Steward O. Quantitative assessment of deficits and recovery
681 of forelimb motor function after cervical spinal cord injury in mice. Exp Neurol 190,
682 184-191 (2004).

683

684 **Acknowledgements**

685 We are grateful for Mariko Hanano (The Jikei University), Ikue Hiraga (Juntendo University)

686 and the Laboratories of Molecular and Biochemical Research, Research Support Center
687 (Juntendo University), for their technical support. This work was supported in part by the Japan
688 Society for the Promotion of Sciences KAKENHI (grant Number 19K07306, 19H03198 and
689 20H04511 to T.Y., 20K11368 to T.K., 19K07105 to N.K., and 19H03404 to T.M.), the USA
690 National Institute of Arthritis, Musculoskeletal and Skin Diseases (R01AR068897; P.D.A.,
691 J.R.L., C.D. and X.L.), the Platform Project for Supporting Drug Discovery and Life Science
692 Research (Basis for Supporting Innovative Drug Discovery and Life Science Research
693 (BINDS)) (JP20am0101098 to H.K. (support number 1858), JP20am0101085 to K.N.,
694 JP20am0101123 to S.N. (support number 1424), and JP20am0101080 to T.M.), the Practical
695 Research Project for Rare/Intractable Diseases (19ek0109202 to N.K.) from the Japan Agency
696 for Medical Research and Development (AMED), and an Intramural Research Grant (29-4 and
697 2-5 to I.N. and T.M., 30-9 and 2-6 to S.Noguchi) for Neurological and Psychiatric Disorders of
698 NCNP, the Vehicle Racing Commemorative Foundation to T.M, and Cooperative Research
699 Project of the Research Center for Biomedical Engineering to H.K..
700

701 **Conflict of Interest**

702 The authors declare that they have no conflict of interest.

703

704 **Author contributions**

705 T.Y., T.K., N.K. and T.M. concepted and designed the work. T.Y., T.K., N.K., M.K., S.Noguchi.,
706 T.I., Y.U.I., S.M., H.I., N.M., A.U., J.A., J.R.L, X.L., C.D., S.K., K.I., B.L., Y.I., K.N. and T.M.
707 acquired and analyzed data. T.Y., T.K., N.K., M.K., S.Noguchi, T.I., Y.U.I., I.N., S.M., H.I.,
708 N.M., H.K., A.U., J.A., J.R.L., X.L., C.D., P.D.A., S.K., K.I., B.L., Y.I., K.N., S.Nakagawa, T.S.
709 and T.M. interpreted data. T.Y., T.K., N.K., S.K., J.R.L, P.D.A. and T.M. wrote and revised the
710 manuscript. All authors reviewed the manuscript.

711 **Figure legends**

712

713 **Fig. 1. Generation and characterization of *RYR1*-p.R2509C (R2509C) mice.** R2509C mice
714 were generated by CRISPR/Cas9 system using single-stranded donor oligonucleotide carrying
715 *Xba* I restriction site (TCTAGA). **a.** Sequences of an amplified DNA fragment from a tail of
716 WT, heterozygous (Hetero), and homozygous (Homo) offspring. Sequencing confirms the
717 presence of both the R2509C mutation and a *Xba* I site on both alleles in homozygous and on
718 one allele in heterozygous offspring. **b.** Gross morphology and allele-specific PCR-RFLP
719 analysis of WT, heterozygous, and homozygous embryos at E19 day. *Top*, Heterozygous
720 embryos (No. 5, 7 and 8) showed no apparent differences from WT embryos (No. 3, 4 and 6),
721 but homozygous embryos (No. 1 and 2) were dead. *Bottom*, presence of a single 688 bp band
722 denotes WT mice, 366 bp and 326 bp bands (not well separated in this gel) denote homozygous
723 mice, and all three bands denote heterozygous mice. **c.** Change in rectal temperature of mice
724 after isoflurane challenge. Heterozygous R2509C mice but not WT mice exhibited elevation in
725 rectal temperature and died by fulminant MH crisis (†). *Inset*, R2509C mice responded with
726 full body contractions as reflected in arching of their backs and extension of their legs. **d.**
727 Maximum rectal temperature of WT (n=8) and R2509C (n=16) mice during isoflurane
728 challenge. *$p < 0.05$ compared to WT. **e.** Time to death from the start of isoflurane challenge or
729 from rectal temperature of 39°C. **f-i.** Comparison between male and female R2509C mice
730 during isoflurane challenge. **f.** Responsiveness to isoflurane. Whereas 90% of male mice
731 increased the body temperature to >39°C, only 65% of female mice exceeded 39°C. **g.**
732 Maximum rectal temperature. **h.** Time to death from isoflurane challenge. **i.** Time to death from
733 rectal temperature of 39°C during isoflurane challenge. There was no difference in this
734 measurement between male and female mice.

735

736 **Fig. 2. Intracellular Ca^{2+} signals in single FDB muscle cells isolated from WT and**
737 **R2509C mice. a.** Structure of Cpd1 sodium salt. **b.** Representative Ca^{2+} signals in the isolated
738 FDB muscle cells from WT and R2509C mice at various concentrations of halothane in the
739 absence (WT and R2509C) and presence of 0.1 μM Cpd1 (R2509C, Cpd1). Fluorescence
740 Ca^{2+} signals (F) were detected with Cal520 and normalized to the initial value (F_0). **c.** Average
741 resting Ca^{2+} signals at various concentrations of halothane and effects of 0.1 μM Cpd1. Data
742 are means ± SD (WT: n=4, R2509C: n=7, R2509C, Cpd1: n=5). *p <0.05 compared to WT.
743 #p <0.05 compared to R2509C. **d.** Average Ca^{2+} signals obtained with fura-2 at rest and in the
744 presence of Cpd1. Data are means ± SD (WT: n=16-34; R2509C: n=17-45). *p <0.05
745 compared to WT. #p <0.05 compared to R2509C. **e.** Representative fura-2 Ca^{2+} ratio signals
746 in isolated FDB muscle cells from WT and R2509C mice at various concentrations of
747 isoflurane in the absence (WT and R2509C) and presence of 0.1 μM Cpd1 (R2509C, Cpd1). **f.**
748 Average resting Ca^{2+} signals at various concentrations of isoflurane and effects of 0.1 μM
749 Cpd1. Data are means ± SD (WT: n=11; R2509C: n=8-10, 2 cells died after exposure to 0.5%
750 isoflurane; R2509C, Cpd1: n=11). *p <0.05 compared to WT. #p <0.05 compared to R2509C.
751
752 **Fig. 3. Contractile function in soleus muscles from WT and R2509C mice. a**. Typical
753 traces of basal stress after exposure to caffeine. Caffeine at indicated concentrations was
754 applied for 2 min. Soleus muscles from R2509C mice exhibit much greater increase in basal
755 stress after exposure to caffeine than those from WT mice. Pretreatment of muscles with Cpd1
756 (3μM) effectively reduces the increase in basal stress caused by caffeine in R2509C muscles.
757 **b**. Dose-dependence of the increase in basal stress in response to caffeine exposure. Means
758 with individual data points are shown (n=5). *p<0.05 compared to WT. **c**. Typical traces of
759 basal stress with increased temperature. **d**. The averaged values of basal stress for 30 seconds
760 after exposure to 42°C. Means with individual data points are shown (n=5). *p<0.05

761 compared to WT. #p<0.05 compared to R2509C. **e**. Typical traces of tension development by
762 electrical stimuli. Muscles were stimulated with 0.5 Hz pulses to evoke twitch and at 1 min
763 intervals with subsequent 20 trains of 1, 2, 5, 10, 20, 50, 100, and 200 Hz pulses. **f**. Summary
764 of twitch tension. Means with individual data points are shown (n=5). No significant
765 difference was observed between WT and R2509C muscles. Cpd1 (3μM) significantly
766 reduces twitch tension. &p<0.05 compared to WT. #p<0.05 compared to R2509C. **g**. Stress-
767 frequency relationship. Data are means ± SD (n=5). No significant difference was observed
768 between WT and R2509C muscles. Cpd1 (3μM) significantly reduces tetanic stress in both
769 groups. & p<0.05 compared to WT. #p<0.05 compared to R2509C.
770
771 **Fig. 4. *In vivo* isoflurane challenge in WT and R2509C mice. A-C.** Preventive effects of
772 Cpd1. **a.** Rectal temperature in mice after anesthesia by isoflurane. Cpd1 (0, 3, 10 mg/kg) was
773 administered *i.p.* to R2509C mice 10 min before anesthesia. †, death by fulminant MH crisis.
774 **b.** Maximum rectal temperature. Data are means ± SD (WT: n=6; R2509C, 0 mg/kg: n=9;
775 R2509C, 3 mg/kg: n=6; R2509C, 10 mg/kg: n=5). *p <0.05 compared to WT. #p <0.05
776 compared to R2509C, 0 mg/kg. **c.** Survival rate of mice after 90 min of anesthesia.
777 Administration of Cpd1 at 10 mg/kg but not 3 mg/kg prevented R2509C mice from fulminant
778 MH crisis. **d-f.** Rescue effects of Cpd1 on fulminant MH crisis in R2509C mice. **d.** Rectal
779 temperature in mice after administration of Cpd1 during anesthesia. Mice were anesthetized
780 by isoflurane and Cpd1 (0, 3, 10 mg/kg) was administered *i.p.* when their body temperature
781 reached 39°C (arrow). †, death by fulminant MH crisis. **e.** Change in rectal temperature of
782 R2509C mice from 39°C at 10 min after the administration of Cpd1 or saline control and the
783 endpoint (60 min after administration or just before death). Data are means ± SD (0 mg/kg:
784 n=16; 3 mg/kg: n=10; 10 mg/kg: n=8). #p <0.05 compared to 0 mg/kg. **f.** Survival rate of
785 R2509C mice 60 min after administration of Cpd1 or Saline control.

786

787 **Fig. 5. *In vivo* heat stress challenge in WT and R2509C mice.** Anesthetized mice were
788 placed in a test chamber prewarmed at 35°C. Cpd1 (10 mg/kg) was administered 10 min
789 before heat stress challenge. **a.** Rectal temperature of mice. **b.** Maximum rectal temperature.
790 Data are means±SD (WT: n=7; R2509C, 0 mg/kg: n=13; R2509C, 10 mg/kg: n=4). *p <0.05
791 compared to WT. **c.** Survival rate of mice 120 min after heat stress challenge. **d.** Time to death
792 from start of heat stress challenge. Data are means±SD (0 mg/kg: n=13; 10 mg/kg: n=4). #p
793 <0.05 compared to 0 mg/kg. **e-g.** Rescue effects of Cpd1 on heat stroke in R2509C mice. **e.**
794 Rectal temperature of mice. Cpd1 (0, 3, 10 mg/kg) was administered *i.p.* when their body
795 temperature reached 39°C (arrow). †, death by heat stroke. **e.** Change in the rectal temperature
796 from 39ºC at 10 min after the administration of Cpd1 or saline control and the endpoint (60
797 min after administration or just before death). Data are means ± SD (0 mg/kg: n=12; 3 mg/kg:
798 n=5; 10 mg/kg: n=11). #p <0.05 compared to 0 mg/kg. **f.** Survival rate of R2509C mice 60
799 min after administration of Cpd1 or saline control.

800

801 **Fig. 6. Pharmacokinetics of Cpd1 in mice. a.** Average plasma concentration-time profiles of
802 Cpd1 following *i.p.* injection of 3 mg/kg and 10 mg/kg. Data are means±SD (n=6 per time
803 point). **b.** Metabolic stability of Cpd1 in the presence of mouse (black) or human (red) liver
804 microsomes. Residual rates of Cpd1 at 0 min were considered 100%. Data are means±SD
805 (mouse: n=7; human; n=4). **c.** Effect of Cpd1 on muscle force of WT mice *in vivo*. Muscle
806 force was measured by grip force test (4-grips test). The tests were performed before (pre) and
807 10 and 60 min after *i.p.* injection of saline or Cpd1. The force values were normalized by
808 body weight (BW). Data are means±SD (n=14). #*p*<0.05, compared to the value of saline-
809 injected control. **d-f**, Effect of repeated administration of Cpd1 on rectal temperature of
810 R2509C mice stimulated by isoflurane (**d**) or environmental heat stress (**e**). Cpd1 was *i.p.*

811 injected 8 times at 1 mg/kg every 10 min and stimulus (isoflurane or environmental heat) was
812 started at time 0. **f.** Survival rate of mice 90 min after isoflurane or heat stress challenge. All
813 the mice survived. **g.** Averaged plasma concentration-time profiles of Cpd1 following 8-times
814 injection of 1 mg/kg at 10 min intervals in male and female mice. Data are means±SD (n=3
815 per time point). **h.** Effect of Cpd1 on muscle force of WT mice *in vivo* following 8-times
816 injection of 1 mg/kg at 10 min intervals. Data are means±SD (n=3).
817
818 **Fig. 7. Effect of Cpd1 on heterozygous *RYR1*-p.R163C (R163C) mice.** Resting $[Ca^{2+}]_i$ in
819 *vastus lateralis* muscle from R163C mice was determined *in vivo* by Ca^{2+} selective
820 microelectrode. **a-d.** Preventive effect of Cpd1. **a.** Effect of Cpd1 on resting $[Ca^{2+}]_i$ in WT and
821 R163C mice with no stimulus. **b.** Time course of $[Ca^{2+}]_i$ in R163C mice during isoflurane
822 challenge. Cpd1 (10 mg/kg) was injected *i.p.* at 20 min and isoflurane was administered at 50
823 min. **c.** Effect of Cpd1 on resting $[Ca^{2+}]_i$ during 1.5% isoflurane anesthesia. Cpd1 dose-
824 dependently reduced $[Ca^{2+}]_i$ in R163C mice to a level in WT mice. Data are means±SD
825 (n=15-21). *p <0.05 compared to WT. #p <0.05 compared to 0 mg/kg Cpd1. **d.** Survival
826 curves of R163C mice after isoflurane anesthesia. Cpd1 dose-dependently increases the
827 survival rate. **e-f**. Rescue effect of Cpd1. **e.** Resting $[Ca^{2+}]_i$ of R163C muscle was determined
828 by Ca^{2+} selective microelectrode. Isoflurane was administered at 20 min and Cpd1 (10 mg/kg)
829 was *i.p.* injected at 35 min. **f.** Summary of resting $[Ca^{2+}]_i$ before (Before) and after exposure
830 to isoflurane (ISF) and after addition of Cpd1 (ISF+Cpd1) in WT and R163C muscles. Cpd1
831 effectively reduces $[Ca^{2+}]_i$ in R163C muscles to the level in WT muscles. Data are means±SD
832 (n=16-20). *p <0.05 compared to WT. #p <0.05 compared to ISF.
833
834 **Fig. 8. Effect of Cpd1 on homozygous *RYR1*-p.G2435R (G2435R) mice. a-b.** *In vivo* heat
835 challenge of G2435R mice. Mice were placed in a 38°C test chamber. Compound 1 (0 or 30

836 mg/kg) was administered *i.p.* 10 min before heat challenge. **a.** Rectal temperature of mice.
837 The steepest and least steep representative rectal temperature changes from 0 mg/kg and 30
838 mg/kg Compound 1 administered mouse groups are shown. **b.** Slope of temperature change
839 from onset to end-point at 40°C. Data are means ± SD (0 mg/kg: n=7; 30 mg/kg: n=5). #p
840 <0.05 compared to 0 mg/kg. **c-d.** Divalent cation entry was measured by Mn^{2+} quench assay
841 with isolated FDB muscle fibers. **c.** Change in fura-2 fluorescence by switching to 1 mM
842 Mn^{2+} containing external solution. The trace for G2435R with 10 μM Cpd1 almost
843 overlapped with that for WT. **d.** Box whisker plots of the slope of the decline in fura-2
844 fluorescence (f.a.u./s) after switching to 1 mM Mn^{2+} containing external solution. G2435R
845 fibers show faster Mn^{2+} entry than WT fibers, an indicative of enhanced divalent cation entry.
846 Cpd1 reduces the rate of Mn^{2+} entry in G2435R fibers in a dose-dependent manner to the
847 level seen in WT fibers. Data are given as box and whisker plots (WT: n=78; G2435R, 0 μM:
848 n=73; G2435R, 1 μM: n=39; G2435R, 10 μM: n=60). *p <0.05 compared to WT. #p <0.05
849 compared to G2435R, 0 μM Cpd1.
850

851 **Table 1. Solubilities of Cpd1 sodium salt and dantrolene sodium salt in solutions for**

852 **injection.**

853

	Cpd1 sodium salt	Dantrolene sodium salt
Normal saline (0.9% NaCl)	849±58 (4)	25.7±2.1 (3)
Pure water	1,360±220 (4)	762±67 (3)
Glucose solution (5%)	351±14 (4)	744±22 (3)

854 *Values are represented in μg/mL.

855 **Number of tests are indicated in parenthesis.

Fig. 1

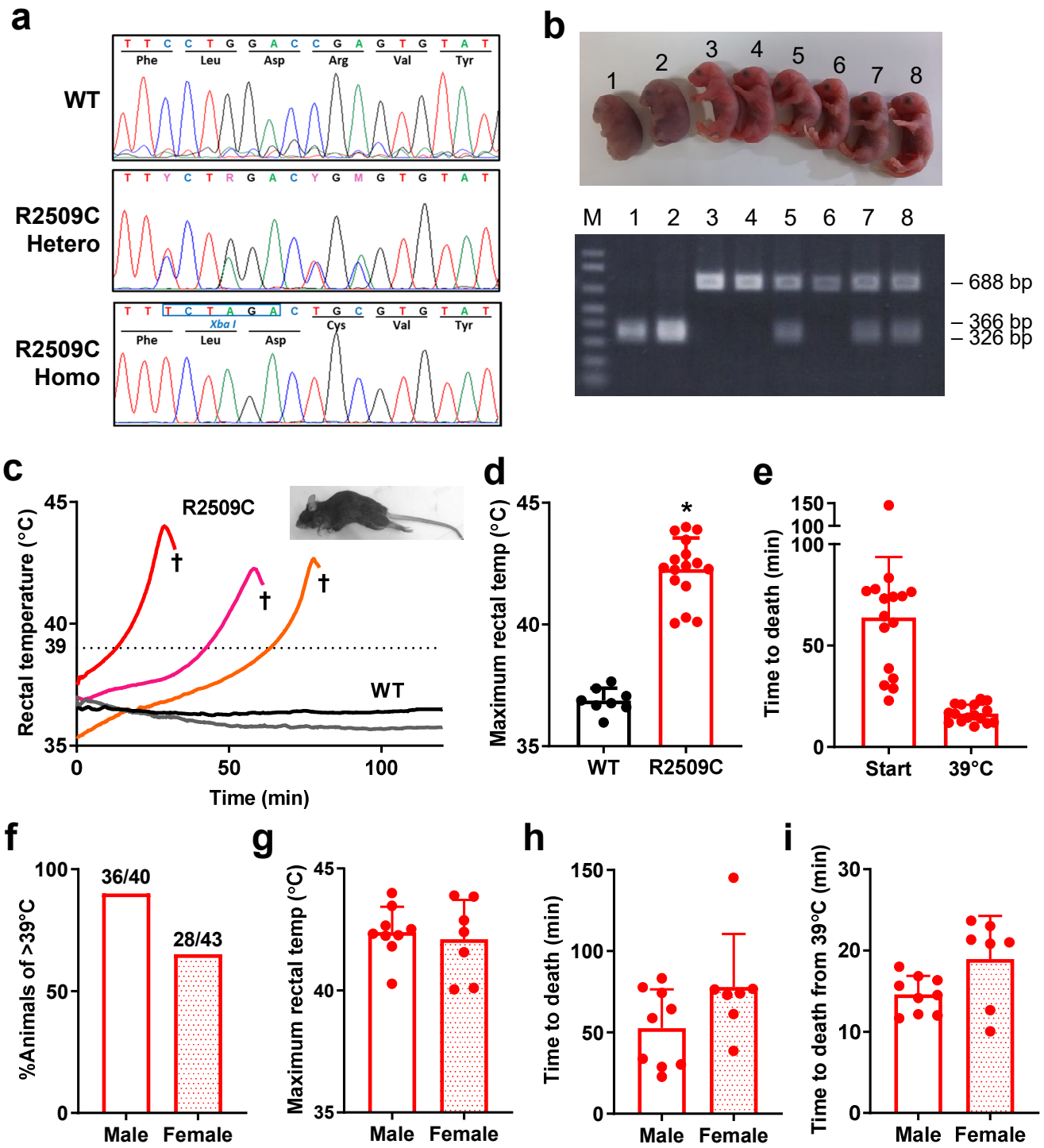
a
WT
R2509C Hetero
R2509C Homo
Phe
Leu
Asp
Arg
Val
Tyr
Xba I
Cys
b
1
2
3
4
5
6
7
8
M
– 688 bp
– 366 bp
– 326 bp
c
R2509C
WT
Rectal temperature (°C)
Time (min)
d
Maximum rectal temp (°C)
WT
R2509C
e
Time to death (min)
Start
39°C
f
%Animals of >39°C
36/40
28/43
Male
Female
g
Maximum rectal temp (°C)
Male
Female
h
Time to death (min)
Male
Female
i
Time to death from 39°C (min)
Male
Female

Fig. 2

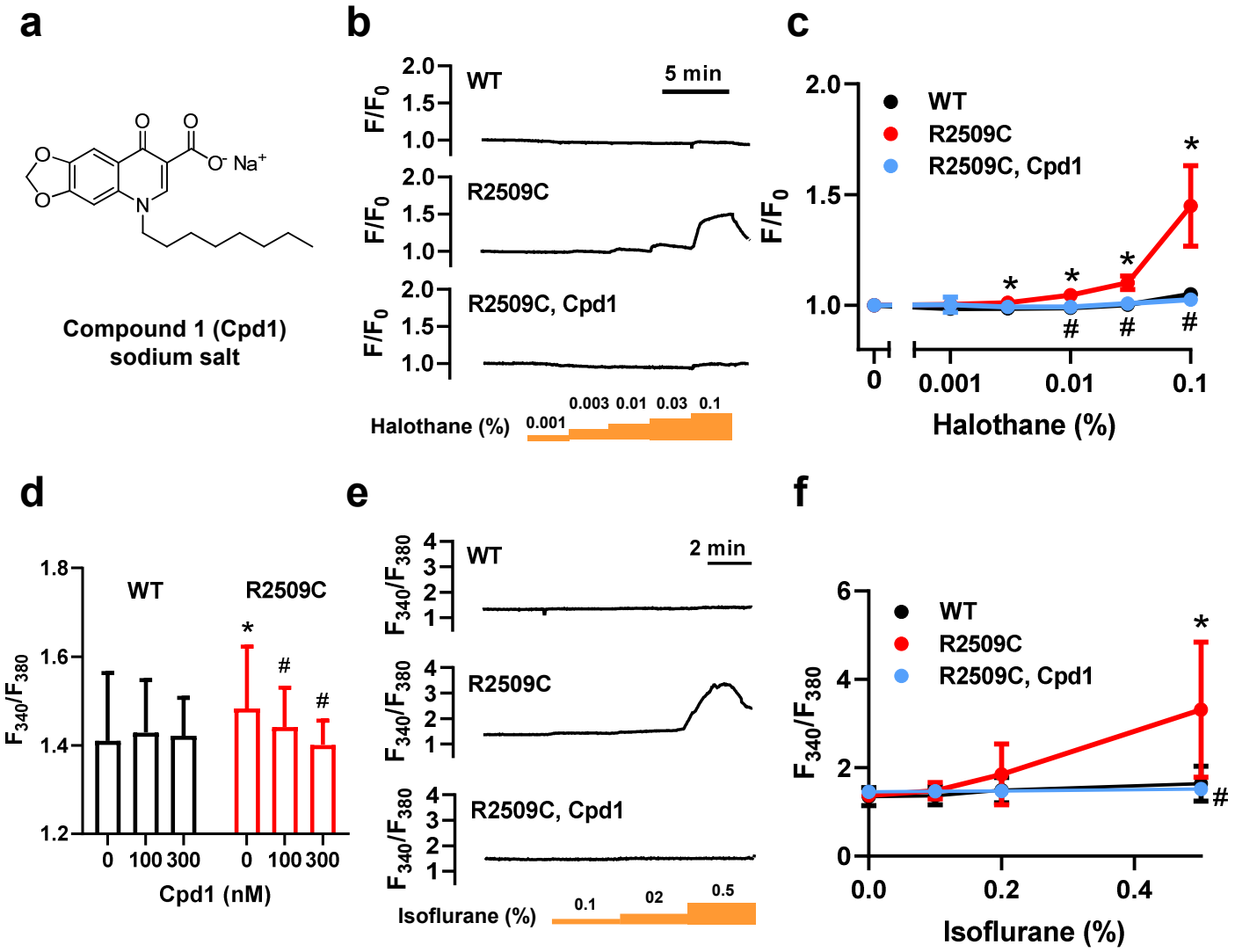
a
Compound 1 (Cpd1)
sodium salt
b
WT
R2509C
R2509C, Cpd1
5 min
F/F0
Halothane (%)
0.001
0.003
0.01
0.03
0.1
c
WT
R2509C
R2509C, Cpd1
F/F0
Halothane (%)
d
WT
R2509C
F340/F380
Cpd1 (nM)
e
WT
R2509C
R2509C, Cpd1
2 min
F340/F380
Isoflurane (%)
0.1
02
0.5
f
WT
R2509C
R2509C, Cpd1
F340/F380
Isoflurane (%)

Fig. 3

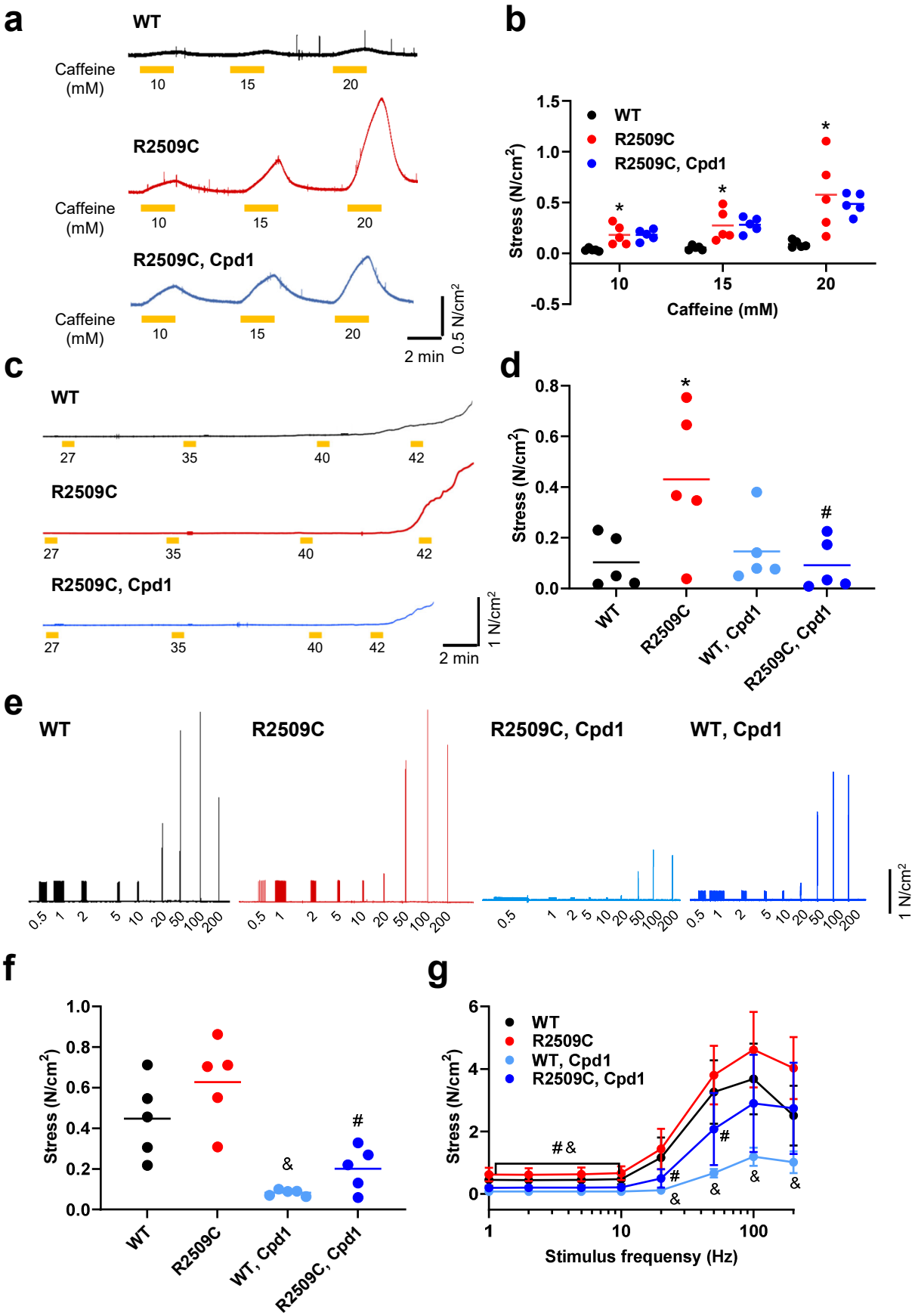
a
WT
Caffeine (mM)
10
15
20
R2509C
R2509C, Cpd1
0.5 N/cm²
2 min
b
WT
R2509C
R2509C, Cpd1
Stress (N/cm²)
Caffeine (mM)
c
27
35
40
42
1 N/cm²
d
WT, Cpd1
e
0.5
1
2
5
10
20
50
100
200
f
g
Stimulus frequensy (Hz)

Fig. 4

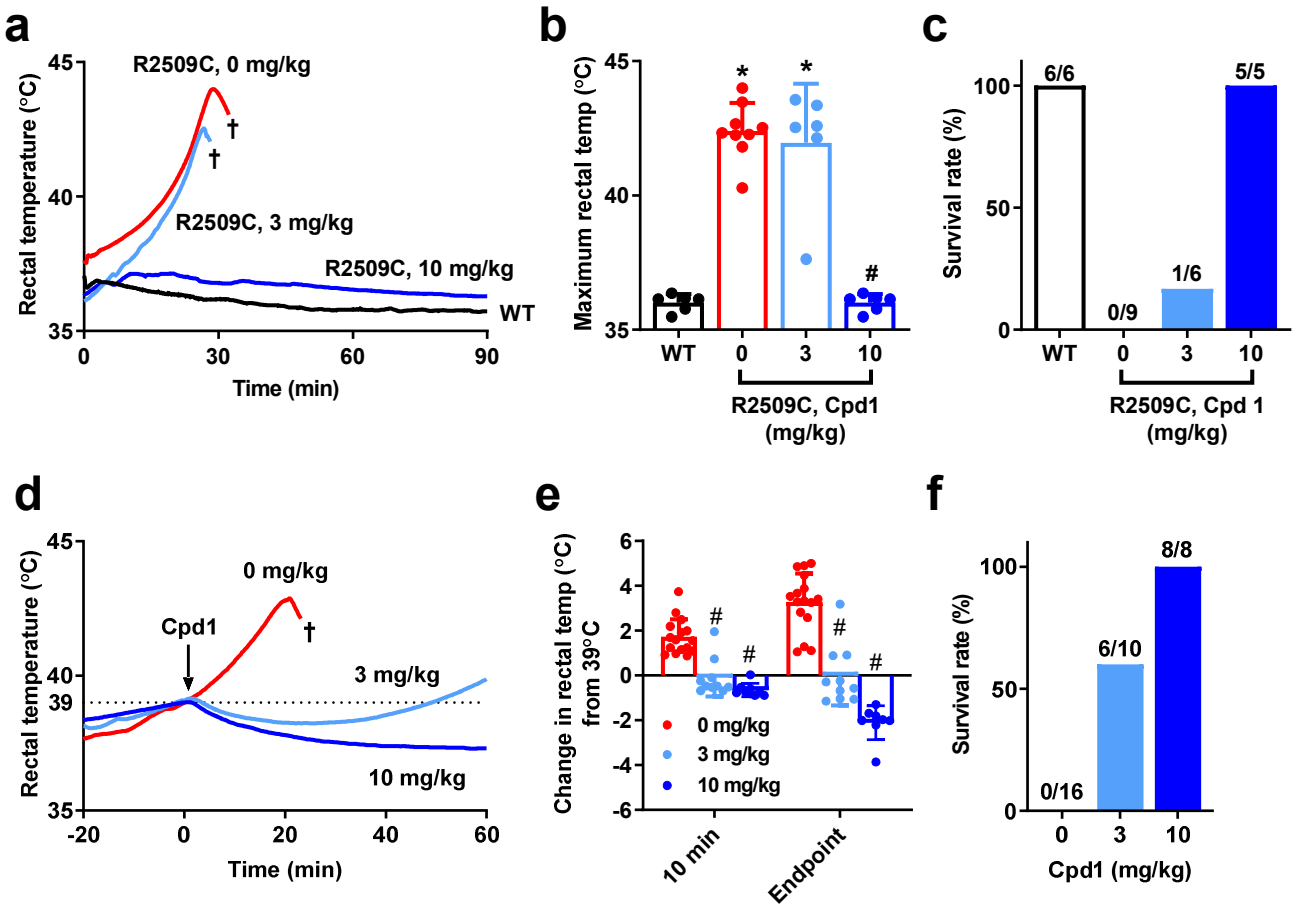
a
R2509C, 0 mg/kg
R2509C, 3 mg/kg
R2509C, 10 mg/kg
WT
Rectal temperature (°C)
Time (min)
b
Maximum rectal temp (°C)
WT
R2509C, Cpd1 (mg/kg)
c
Survival rate (%)
6/6
0/9
1/6
5/5
R2509C, Cpd 1 (mg/kg)
d
0 mg/kg
Cpd1
3 mg/kg
10 mg/kg
Rectal temperature (°C)
Time (min)
e
Change in rectal temp (°C) from 39°C
0 mg/kg
3 mg/kg
10 mg/kg
10 min
Endpoint
f
Survival rate (%)
0/16
6/10
8/8
Cpd1 (mg/kg)

Fig. 5

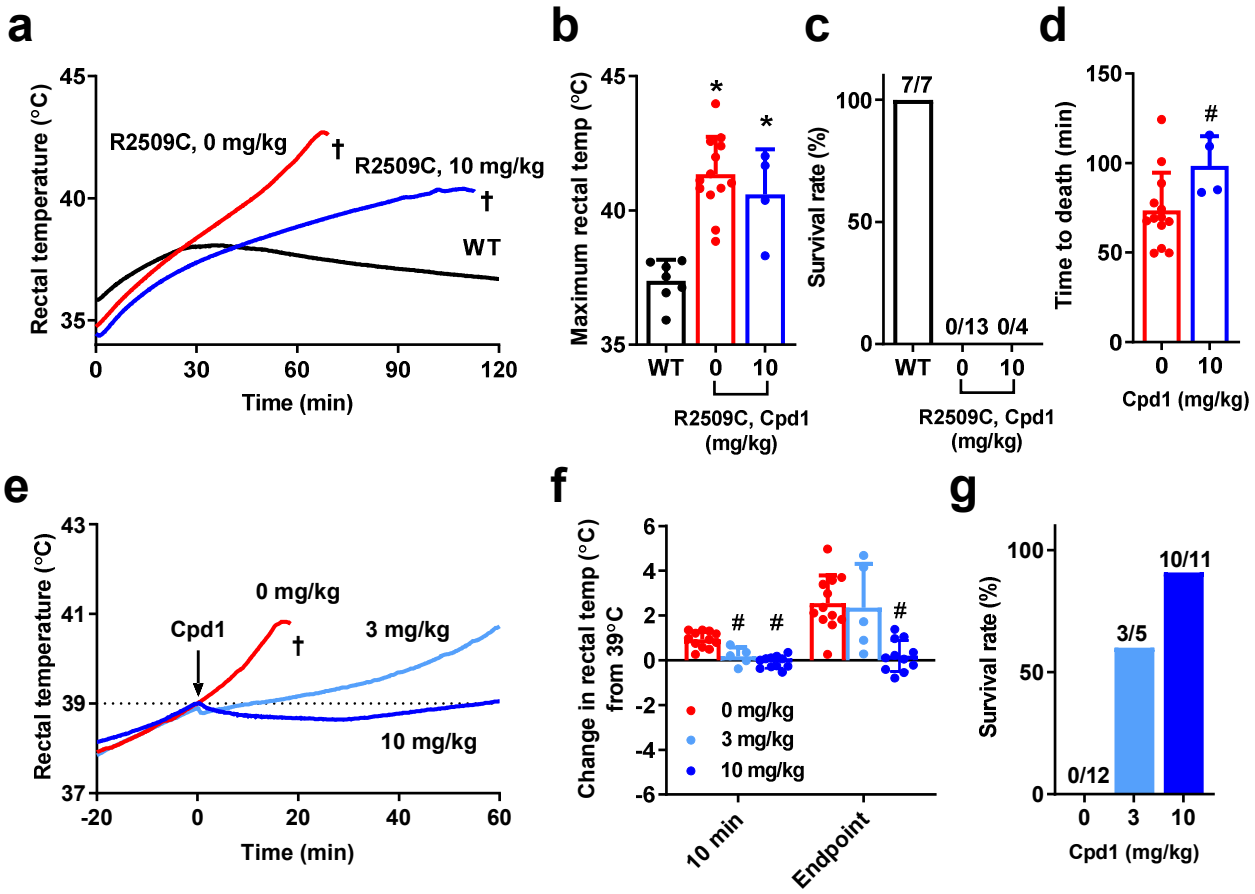
a
Rectal temperature (°C)
R2509C, 0 mg/kg
R2509C, 10 mg/kg
WT
Time (min)
b
Maximum rectal temp (°C)
WT
R2509C, Cpd1 (mg/kg)
c
Survival rate (%)
7/7
0/13 0/4
WT
R2509C, Cpd1 (mg/kg)
d
Time to death (min)
Cpd1 (mg/kg)
e
Rectal temperature (°C)
0 mg/kg
Cpd1
3 mg/kg
10 mg/kg
Time (min)
f
Change in rectal temp (°C) from 39°C
0 mg/kg
3 mg/kg
10 mg/kg
10 min
Endpoint
g
Survival rate (%)
0/12
3/5
10/11
Cpd1 (mg/kg)

Fig. 6

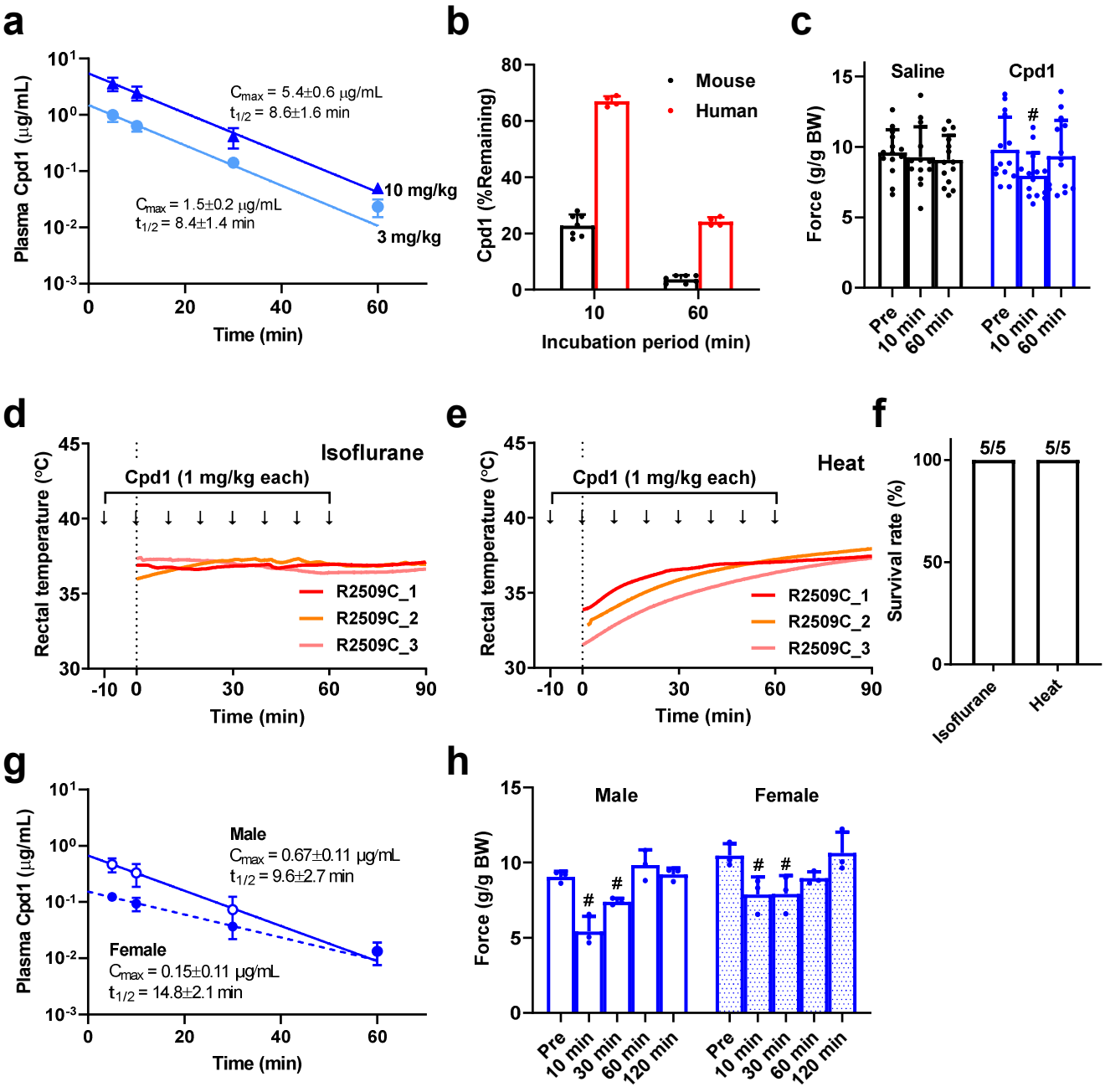
a
Plasma Cpd1 (μg/mL)
Time (min)
Cmax = 5.4±0.6 μg/mL
t1/2 = 8.6±1.6 min
10 mg/kg
Cmax = 1.5±0.2 μg/mL
t1/2 = 8.4±1.4 min
3 mg/kg
b
Cpd1 (%Remaining)
Mouse
Human
Incubation period (min)
c
Saline
Cpd1
Force (g/g BW)
Pre
10 min
60 min
d
Isoflurane
Cpd1 (1 mg/kg each)
Rectal temperature (°C)
R2509C_1
R2509C_2
R2509C_3
Time (min)
e
Heat
Cpd1 (1 mg/kg each)
Rectal temperature (°C)
R2509C_1
R2509C_2
R2509C_3
Time (min)
f
Survival rate (%)
5/5
5/5
Isoflurane
Heat
g
Plasma Cpd1 (μg/mL)
Male
Cmax = 0.67±0.11 μg/mL
t1/2 = 9.6±2.7 min
Female
Cmax = 0.15±0.11 μg/mL
t1/2 = 14.8±2.1 min
Time (min)
h
Male
Female
Force (g/g BW)
Pre
10 min
30 min
60 min
120 min

Fig. 7

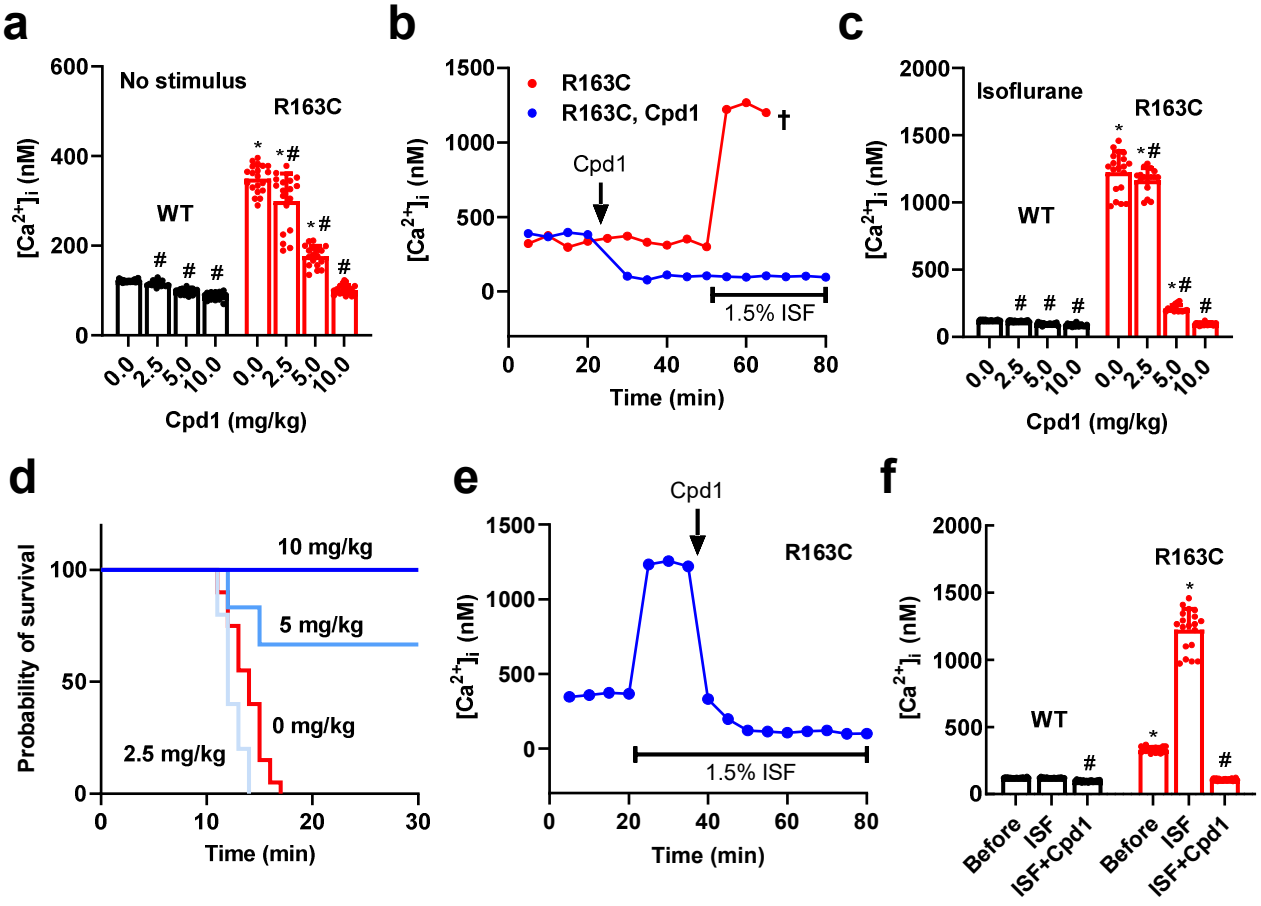
a
No stimulus
R163C
WT
[Ca2+]i (nM)
Cpd1 (mg/kg)
b
R163C
R163C, Cpd1
Cpd1
1.5% ISF
[Ca2+]i (nM)
Time (min)
c
Isoflurane
R163C
WT
[Ca2+]i (nM)
Cpd1 (mg/kg)
d
10 mg/kg
5 mg/kg
0 mg/kg
2.5 mg/kg
Probability of survival
Time (min)
e
Cpd1
R163C
1.5% ISF
[Ca2+]i (nM)
Time (min)
f
R163C
WT
[Ca2+]i (nM)
Before
ISF
ISF+Cpd1

Fig. 8

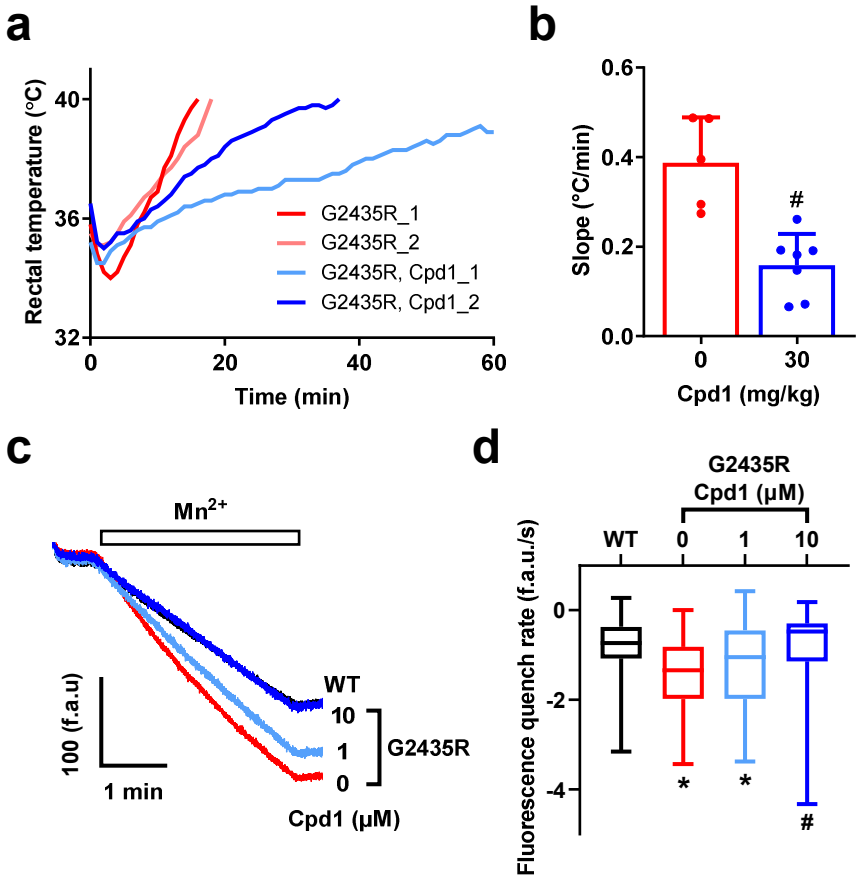
a
Rectal temperature (°C)
40
36
32
0
20
40
60
Time (min)
G2435R_1
G2435R_2
G2435R, Cpd1_1
G2435R, Cpd1_2
b
Slope (°C/min)
0.6
0.4
0.2
0.0
#
0
30
Cpd1 (mg/kg)
c
Mn2+
100 (f.a.u)
1 min
WT
10
1
0
G2435R
Cpd1 (μM)
d
G2435R
Cpd1 (μM)
WT
0
1
10
Fluorescence quench rate (f.a.u./s)
0
-2
-4
*
*
#